Electrical Power and Energy Systems 172 (2025) 111171

Contents lists available at ScienceDirect

International Journal of Electrical Power and Energy Systems

journal homepage: www.elsevier.com/locate/ijepes

A joint bidding mode for charging stations approaching social welfare maximization☆,☆☆

Gaojunjie Li [a], Huiying Li [b], Fuzhang Wu [c,*], Xiangpeng Zhan [d], Xiang Gao [e]

[a] Department of Electrical and Electronic Engineering, Hong Kong Polytechnic University, Kowloon, Hong Kong Special Administrative Region of China
[b] Department of Land Surveying and Geo-Informatics, Hong Kong Polytechnic University, Kowloon, Hong Kong Special Administrative Region of China
[c] School of Electrical Engineering and Automation, Wuhan University, Wuhan, Hubei, China
[d] State Grid Fujian Marketing Service Center (Metering Center), Fuzhou, Fujian, China
[e] Development and Construction Department, Guilin Division, Guangxi Guiguan Electric Power Co., Ltd., Guilin, Guangxi, China

ARTICLE INFO

Keywords:
Electric vehicles
Electricity market
Day-ahead bidding
Distributed algorithm
Social welfare

ABSTRACT

Megawatt supercharger stations will act as price-makers due to their large charging capacity. However, charging station operators (CSOs) have different accuracy in forecasting clearing price. Disordered bidding caused by asymmetry information will cause unnecessary social welfare loss. For this, a joint bidding mode that is easy to apply and approaches social welfare maximization is proposed. A third-party operator (TPO) is introduced as an assistant of the market operator to joint and coordinate CSOs, while retaining the local checking role of the distribution system operator (DSO). Little private information is exchanged to coordinate a large number of multi-region CSOs to bid on the premise of considering the interests of all players and the operation of both transmission and distribution systems. Graphical method is used to prove that the TPO can adjust the lower bound of bid/offer price of CSOs to approach the social welfare maximum. Taking the three-month load data of the UK power grid as a case, the deviation is concentrated in the interval [6.2%, 13.5%], with a minimum deviation of only 2.1%.

1. Introduction

Nowadays, the popularity of electric vehicles (EVs) has led to a strong demand for charging [1]. Supercharger stations with 72 and 56 charging piles have been built in Shanghai, China and Fresno County, California, USA respectively [2]. And the maximum peak power of piles are 150 kW and 250 kW respectively. There will be more such charging stations (CSs) in the future. Based on the flexible charging and discharging characteristics of electric vehicles, charge station operators (CSOs) aggregate EVs and act as large prosumers on the user side, i.e., switching between consumers and producers [3–5]. To further stimulate market vitality, Order No. 719 of the FERC [6] and the EU energy efficiency directives [7] allow consumers to participate in market transactions alone or through load aggregators. In Sept. 2020, Order No. 2222 of the FERC [8] reduced the minimum market access capacity to 100 kW. Obviously, the supercharger stations fully meet the access threshold. Meanwhile, since EVs give CSs great flexibility [9], large enough charging demand and discharge capacity make CSOs different from traditional price-takers, and able to participate in the market as price-makers with certain market rights [10,11]. At this point, the influx of a large number of CSs into the market is bound to increase the complexity and risk of market transactions.

As a profit-making price-maker, the CSO with market power hopes to benefit from influencing the market clearing price [12]. In the unified clearing wholesale market [13], when bidding independently, the CSO mainly formulate its bidding strategy through price forecasting based on price sensitivity [14,15]. However, in the China's actual market with imperfect competitive and asymmetric information [16], the predictable information of CSOs may be limited to other local players. This results in the inaccurate forecasted clearing price and blind bidding strategies of CSOs. Even if the price uncertainty is considered when single player formulates its bidding strategy [17,18], the improvement effect is limited by risk appetite of players and the social welfare of the whole market will not be substantially improved. Then, if the actual market is not coordinated, disordered competition among

☆ This article is part of a Special issue entitled: 'EV Integration and V2G Interaction' published in International Journal of Electrical Power and Energy Systems.
☆☆ This work was supported in part by the MOE (Ministry of Education in China) Project of Humanities and Social Sciences under Grant 24YJCZH337 and the National Natural Science Foundation of China under Grant 52507141.
* Corresponding author.
E-mail addresses: gaojunjie.li@polyu.edu.hk (G. Li), huihuiying.li@connect.polyu.hk (H. Li), wfzhang@whu.edu.cn (F. Wu), xiangpengzhan@whu.edu.cn (X. Zhan), 509809007@qq.com (X. Gao).

https://doi.org/10.1016/j.ijepes.2025.111171
Received 2 April 2025; Received in revised form 11 September 2025; Accepted 18 September 2025
Available online 1 October 2025

Nomenclature

Indices and sets

b	Index of generation blocks.
g/d	Index of generator/load in transmission system.
$e/v/w$	Index of EVs/CSOs/DSOs.
i/j	Index of buses in distribution/transmission system.
l	Index of branches in distribution system.
m/n	Index of start/end of branches.
k	Index of iterations.
$\mathbf{T}$	Index of branches in distribution system.
$\mathbf{N}_v^{EV}$	Set of EVs in charging station v.
$\mathbf{V}^w$	Set of charging stations in distribution system w.
$\mathbf{\Omega}^w/\mathbf{L}^w$	Set of buses/branches in distribution system w.
$\mathbf{W}/\mathbf{W}^j$	Set of DSOs/DSOs at bus j.
$\mathbf{N}_{step}$	Set of generation blocks.
$\mathbf{TG}/\mathbf{TL}$	Set of generators/transmission system branches.

Variables

$p_{e,t}^c/p_{e,t}^d$	Charging/discharging power of EV e in period t.
$s_{e,t}$	State of charge of EV e in period t.
$P_{v,t}^c/P_{v,t}^d$	Charging/discharging power of CSO v in period t.
$S_{v,t}$	State of charge of CSO v in period t.
$P_{i,t}^{in}$	Injection power at bus i in period t.
$\lambda_{t,w}^{DA}$	Day-ahead clearing price at DSO w in period t.
$\kappa_{v,t,w}^{DA}$	Bid/offer price of CSO v in period t.
$P_{b,t,g}^G$	Power produced by block b of unit g in period t.
$\theta_{t,j}$	Voltage phase angle at bus j in period t.
π^c/π^d	Lagrange multiplier.
$\lambda_{v,t,w}^{DLMP}$	DLMP in period t sent by DSO w to CSO v.
λ/μ	Dual variables of equality/inequality constraints.
$P_{v,t,w}^{TPOc/d}$	Reference charging/discharging power of CSO v in period t, provided by TPO as reference values for optimizing bidding strategies.
$P_{v,t,w}^{CSc/d}$	Expected charging/discharging power of CSO v in period t, submitted by CSO to TPO as feedback during the iterative coordination process.
$\mu_{l,t}^{+/-}$	Marginal congestion price of branch l in period t.
ψ	Social welfare of market under day-ahead joint bidding mode.

Parameters

$X_{e,t}$	State of EV e in period t.
T_e^a/T_e^d	Arrival/departure time of EV e.
$\overline{p_e^c}/\overline{p_e^d}$	Upper bound of $p_{e,t}^c/p_{e,t}^d$.
$\overline{s_e}/\underline{s_e}$	Upper/lower bound of $s_{e,t}$.
η^c/η^d	Charging/discharging efficiency.
η^{ref}	Discharge compensation coefficient.
Δt	Time interval.
s_e^a/s_e^d	State of charge of EV e at arrival/departure.
$\overline{P_{v,t}^c}/\overline{P_{v,t}^d}$	Upper bound of $P_{v,t}^c/P_{v,t}^d$.
$\overline{S_{v,t}}/\underline{S_{v,t}}$	Upper/lower bound of $S_{v,t}$.
$\Delta S_{v,t}$	Change in $S_{v,t}$ due to EV arrival and departure.
$\mathbf{D}$	Power transfer distribution factor matrix.
α	Iteration step of subgradient method.
ρ	Penalty coefficient.
$P_{i,t}^D$	Base load at bus i in period t.
$\pi_{b,g}^G$	Price offer of block b of generation unit g.
$G_{b,g}$	Capacity of block b of generation unit g.
$\overline{\kappa_{v,t,w}}/\underline{\kappa_{v,t,w}}$	Upper/lower bound of $\kappa_{v,t,w}^{DA}$.
B_{mn}	Susceptance of line $m-n$.
$\overline{F_l}/\overline{F_{mn}}$	Transmission capacity of line $l/m-n$.
$\varepsilon_{pri}/\varepsilon_{dual}$	Primal/dual residuals.

Abbreviations

EV	Electric vehicle.
CS/CSO	Charge station/charge station operator.
DSO	Distribution system operator.
TPO	Third-party operator.
MO	(Wholesale) market operator.
DLMP	Distribution locational marginal pricing.
GNE	Generalized Nash equilibrium.

players with market power will reduce market efficiency. For example, inadvertently increasing prices [19], congestion [20] and adverse selection [21] will lead to market failures. For this reason, a market coordinator for aggregate CSs was introduced to organize joint bidding in [19,22], and the feasibility was discussed in [23]. Through coordinating the energy schedules of CSOs to avoid excessive rise of price during peak load periods, the unnecessary loss caused by disorderly competition under asymmetry information is reduced. However, the coordinator in [20] aims to maximize the benefits of the CS cluster without considering the impact of its bid on the interests of other players and the system operation. It is only the agent of the CSs, not the real market coordinator aiming at maximizing social welfare. In this regard, in the electricity market of Hunan, China, the role of market coordinator is played by the non-profit dispatching organization. Certain market information will be disclosed to CSOs, but they are required to report their charging load curve [24]. This method is conducive to transforming the market to a perfect information market to alleviate disorderly competition. Besides, the user information sharing mode based on block-chain was proposed to improve social welfare in [25]. Therefore, it is necessary to reasonably set up an auxiliary institution to organize and coordinate a large number of CSOs to bid.

The fundamental purpose of coordination is to realize the original intention of establishing the market, that is, to maximize social welfare. However, it is difficult to maximize social welfare under the competition among players with market rights. Therefore, how to design a transaction mechanism that can achieve or approach social welfare maximization in the actual market needs to be studied. Many scholars have studied this problem. To analyze the optimal response of players in an imperfect competition market and determine the optimal bidding strategies to maximize social welfare, a bi-level model was established in [26]. The market player formulated its energy schedule with the goal

of maximizing profit in the upper level, while the market was cleared with the goal of minimizing operation cost in the lower level. The Karush–Kuhn–Tucker (KKT) condition was used to convert the bi-level model into a single-level model. A competitive bidding model under the unified clearing price mode of renewable energy operators was established in [27]. The diagonalization algorithm was used to obtain the Generalized Nash equilibrium (GNE). A generalized Nash game model with multiple price-makers was established in [28]. The optimal Nash equilibrium was obtained by solving the optimality conditions of each price maker simultaneously. Similarly, multi-agent generalized Nash game models of P2P energy trading in active distribution networks and direct trading between micro-grids were established and solved in [29,30], respectively. When many players reach the GNE through a long-term game, all players achieve the best utility and have no desire to deviate [31]. It can be considered that social welfare maximization in an imperfect competitive market has been realized. Similarly, in [32], a holistic risk-aware bi-level optimization framework was proposed for incorporating financial entities into spot electricity markets with renewable energy, analyzing the impacts of risk preferences (averse, neutral, seeking) on day-ahead and real-time market clearing through virtual bidding strategies. This approach highlighted how aggressive bidding could amplify volatility in renewable-dominant markets while providing sensitivity analyses for risk and renewable penetration levels.

However, the above work has the following problems, which are the focus of this paper: (1) Difficult to achieve game equilibrium in the actual market: the KKT condition and diagonalization algorithm are used to obtain the game equilibrium. Using these methods means that the MO needs to obtain the private information of all players and players are allowed to modify their bids/offers repeatedly. This is not allowed in the actual market. Meanwhile, players with market power are more likely to regard any information assets they may have as potential strategic advantages, which they are unwilling to share [33]; (2) The formation cycle of game equilibrium is long: the GNE is the result of a long-term game, which can be seen as an evolutionary game [34]. When new market players join, the equilibrium is bound to be broken, and the formation of a new equilibrium is also a long-term process. (3) Lack of analysis of deviation from maximum social welfare: The existing works only analyze the optimal response of each player from the game perspective. There is no comparison between social welfare under the GNE in the imperfect competition market and maximum social welfare. The causes of deviation are also lack of analysis.

In short, there is no suitable transaction mechanism in the existing works that can applied in the actual market to coordinate a large number of CSOs to bid, so as to achieve or approach the maximum social welfare. Therefore, in this paper, a third-party operator (TPO) is introduced as an assistant of MO to joint and coordinate CSOs to bid. The centralized models that can maximize social welfare are transformed into a distributed model with energy schedules as the interactive variables. Through the interaction among the TPO, CSOs and distribution system operator (DSO) to make the day-ahead clearing results approach the maximum social welfare. Simulations are utilized to validate the method. The main contributions are as follows:

(1) A joint bidding mode of CSOs coordinated by the TPO and local DSOs is designed to reduce social welfare loss and avoid local congestion. The joint bidding mode expands the coordination mechanism proposed in [19] by considering the physical constraints of transmission and distribution systems, and focuses on the social welfare improvement rather than cost reduction. On the premise of considering the interests of all market players and the safe operation of both transmission and distribution systems, little private information, i.e. the energy schedules of CSOs, is used to coordinate a large number of CSOs in multiple regions to bid. Compared to bidding modes based on generalized Nash games in prior works, the proposed mode can be readily implemented in practical market settings due to its distributed framework, which requires minimal information exchange.

(2) A distributed algorithm based on the subgradient method and alternating direction method of multipliers (ADMM) is designed to implement the joint bidding. The algorithm consists of two parallel parts: (a) the interaction algorithm between CSOs and the local DSO based on Lagrangian duality decomposition (LDD). (b) the interaction algorithm between CSOs and the TPO based on the decomposition mechanism of ADMM. Both parts are decomposed by the centralized models aiming at maximizing social welfare, which is the basis for approaching the maximum social welfare. The distributed algorithm retains the market power of CSOs and has good convergence.

(3) The effectiveness of the joint bidding mode is proved. Through the graphical method, it is proved that the TPO can adjust the lower bound of CSOs' bid/offer price to make the joint bidding results approach the social welfare maximum, that is, the social welfare loss can be controlled in a small range. In the simulation, the deviation is concentrated in the interval [6.2%, 13.5%], with a minimum deviation of only 2.1%. The most important reason for approaching the maximum social welfare is that the joint bidding mode helps local CSOs reach a price consensus on the bid/offer. The price consensus avoids the clearing results severely deviating from the expectations because of the blind bidding of CSOs. Meanwhile, the Kaldor–Hicks improvement of CSO cluster benefit is realized.

The rest of this paper is organized as follows. The framework the day-ahead joint bidding mode is clarified in Section 2. The generalized energy storage model of the CSO is established in Section 3. The model, algorithm and related proof of the joint bidding mode are given in Section 4. Illustrative examples are provided in Section 5. A detailed discussion is presented in Section 6. Finally, conclusions are summarized in Section 7.

2. Framework of day-ahead joint bidding mode

As CSOs grasp market information in a short time with difficulty, deviation is inevitable when they forecast the market clearing price. When the deviation is large, it is difficult for CSOs to report appropriate bid/offer prices in the wholesale market to obtain ideal clearing results. The unsatisfactory clearing result will severely deviate from the expectations of CSOs and cause loss. In addition, if many CSOs only consider their own benefits when formulating bidding strategies, they are likely to charge or discharge centrally at some time since they accept the same forecasted clearing price. This situation is bound to cause a positive or reverse load spike, as well as an increased probability of network congestion and unnecessary congestion costs. Therefore, a new joint bidding mode is designed in this paper, as shown in Fig. 1.

The joint bidding mode mitigates the adverse effects of inaccurate market clearing price forecasts by CSOs, which can lead to disordered bidding and social welfare losses. As shown in Fig. 1, the TPO coordinates CSOs in the day-ahead bidding process under the supervision of the MO, similar to coordinators in [19,22,23]. It may be operated by a nonprofit governmental entity or an independent service platform. The TPO accesses precise market data, such as generator offer prices and transmission system parameters, which are not disclosed to CSOs to ensure market fairness. Unlike prior coordinators, this TPO integrates transmission system physical constraints and prioritizes market-wide social welfare in its coordination strategy. Additionally, it employs a distributed interaction framework in Section 4.3, utilizing iterative information exchange of energy schedules rather than centralized data aggregation, enabling scalable coordination across multi-region CSOs.

During joint bidding, the TPO iteratively shares optimized reference energy schedules, including charging and discharging powers $P^{TPOc}_{v,t,w}$ and $P^{TPOd}_{v,t,w}$, derived from solving the wholesale market subproblem SP2 in Section 4.2, with CSOs as reference values. These reference schedules integrate transmission system constraints and generator offer data to minimize overall CSO operating costs while adhering to market clearing conditions. In response, each CSO incorporates these references into its optimization objective (via penalty terms and Lagrange multipliers in

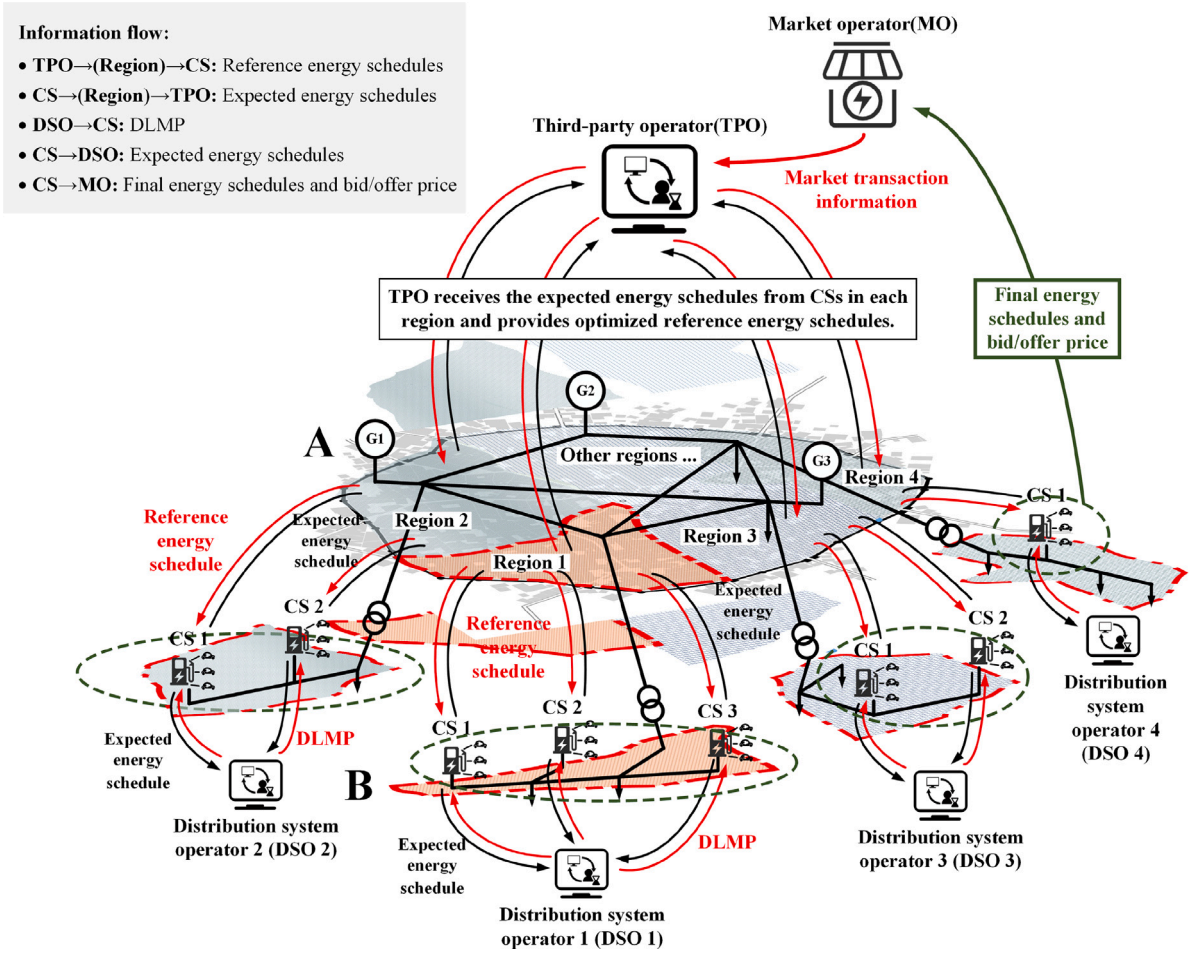

Fig. 1. The framework of the day-ahead joint bidding mode (A: Transmission system; B: Local distribution system).

distribution system subproblem SP1 in Section 4.2), adjusting its own schedules $P^{CSc}_{v,t,w}$ and $P^{CSd}_{v,t,w}$ based on local distribution constraints from DSOs. The updated schedules are then fed back to the TPO, enabling both parties to iteratively converge toward mutual agreement. This process, driven by the ADMM-based algorithm in Section 4.3, continues until the convergence criteria are satisfied, achieving consensus on bid/offer prices $\kappa^{DA}_{v,t,w}$ and schedules that approximates social welfare maximization while exchanging only minimal private information (e.g., energy schedules). Once consensus is reached, CSOs finalize their bidding strategies based on the agreed-upon schedules and prices, submitting a single round of bids/offers in the day-ahead market. The DSO ensures safe and stable operation of the local distribution system by validating CSO schedules against congestion constraints and calculating the distribution locational congestion price (DLMP) through iterative interaction with CSOs. This validation ensures local grid reliability while supporting the TPO's coordination. As CSOs' strategies remain fixed post-consensus, the single-round bidding process enhances market efficiency by reducing iterative adjustments during market clearing.

3. Generalized energy storage model of CSO

The CSO can obtain the probability distribution of the EV arrival time, departure time, initial capacity and expected capacity according to the historical EV charging data, and then predict the charging demand of the next day [35]. In the joint bidding mode, to facilitate the TPO to provide more accurate optimized reference schedules for CSOs, CSOs need to provide the range of charging demand and discharge capacity in each period of the next day. The CSO is modeled as a generalized energy storage device with charging and discharging capabilities. It can completely describe the characteristics of the CSO with little private data to reduce modeling complexity. The detailed modeling process is as follows. The individual model of an EV is as follows:

$$X_{e,t} = 0, \forall t \notin \left[T^a_e, T^d_e\right], X_{e,t} = 1, \forall t \in \left[T^a_e, T^d_e\right] \tag{1}$$

$$0 \le p^c_{e,t} \le \overline{p^c_e} X_{e,t}, \forall e \in \mathbf{N}^{EV}_v, \forall t \in \mathbf{T} \tag{2}$$

$$0 \le p^d_{e,t} \le \overline{p^d_e} X_{e,t}, \forall e \in \mathbf{N}^{EV}_v, \forall t \in \mathbf{T} \tag{3}$$

$$p^c_{e,t} p^d_{e,t} = 0, \forall e \in \mathbf{N}^{EV}_i, \forall t \in \mathbf{T} \tag{4}$$

$$s_{e,t} = X_{e,t}\left(s_{e,t-1} + \eta^c p^c_{e,t}\Delta t - \frac{\eta^{ref} p^d_{e,t}\Delta t}{\eta^d}\right) \tag{5}$$

$$\underline{s_e} X_{e,t} \le s_{e,t} \le \overline{s_e} X_{e,t}, \forall e \in \mathbf{N}^{EV}_i, \forall t \in \mathbf{T} \tag{6}$$

It is proven in Appendix A that when η^c and η^d are not 100%, the EV will not charge and discharge at the same time, so (4) can be ignored. Considering the arrival, departure and access period characteristics of EVs, (5) can be rewritten as follows:

$$\begin{aligned} s_{e,t} = {} & s_{e,t-1} + s^a_e X_{e,t}\left(X_{e,t} - X_{e,t-1}\right) \\ & - s^d_e X_{e,t-1}\left(X_{e,t-1} - X_{e,t}\right) + \eta^c p^c_{e,t}\Delta t - \frac{\eta^{\mathrm{ref}} p^d_{e,t}\Delta t}{\eta^d} \end{aligned} \tag{7}$$

In the model, the definition domain of all EVs is the whole period **T**, so Minkowski addition [36] can be used to address (2)–(3), (6) and

(7). The envelope space is obtained as follows:

$$0 \le \underbrace{\sum_{e\in \mathbf{N}_v^{EV}} p_{e,t}^c}_{\triangleq P_{v,t}^c} \le \underbrace{\sum_{e\in \mathbf{N}_v^{EV}} \overline{p_e^c} X_{e,t}}_{\triangleq \overline{P_{v,t}^c}}, \forall t \in \mathbf{T} \tag{8}$$

$$0 \le \underbrace{\sum_{e\in \mathbf{N}_v^{EV}} p_{e,t}^d}_{\triangleq P_{v,t}^d} \le \underbrace{\sum_{e\in \mathbf{N}_v^{EV}} \overline{p_e^d} X_{e,t}}_{\triangleq \overline{P_{v,t}^d}}, \forall t \in \mathbf{T} \tag{9}$$

$$\begin{aligned} \sum_{e\in \mathbf{N}_v^{EV}} s_{e,t} &= \eta^c \Delta t \sum_{e\in \mathbf{N}_v^{EV}} p_{e,t}^c - \frac{\eta^{ref} \Delta t \sum_{e\in \mathbf{N}_v^{EV}} p_{e,t}^d}{\eta^d} \\ &+ \sum_{e\in \mathbf{N}_v^{EV}} s_{e,t-1} + \underbrace{\sum_{e\in \mathbf{N}_v^{EV}} \begin{pmatrix} s_e^a X_{e,t}\left(X_{e,t} - X_{e,t-1}\right) \\ -s_e^d X_{e,t-1}\left(X_{e,t-1} - X_{e,t}\right) \end{pmatrix}}_{\Delta S_{v,t}} \end{aligned} \tag{10}$$

$$\underbrace{\sum_{e\in \mathbf{N}_v^{EV}} \underline{s_e} X_{e,t}}_{\triangleq \underline{S_{v,t}}} \le \underbrace{\sum_{e\in \mathbf{N}_v^{EV}} s_{e,t}}_{\triangleq S_{v,t}} \le \underbrace{\sum_{e\in \mathbf{N}_v^{EV}} \overline{s_e} X_{e,t}}_{\triangleq \overline{S_{v,t}}} \tag{11}$$

Therefore, the generalized energy storage model of the CSO is shown in (12). The model not only reflects the charging demand and discharge capacity of the CSO in each period but also protects the charging demand privacy of EV owners. CSOs can obtain the model parameters $\left\{\overline{P_{v,t}^c}, \overline{P_{v,t}^d}, \underline{S_{v,t}}, \overline{S_{v,t}}, \Delta S_{v,t}\right\}$ according to the method in (8)–(11) and report them to the TPO.

$$\left\{ \begin{array}{c} 0 \le P_{v,t}^c \le \overline{P_{v,t}^c}, 0 \le P_{v,t}^d \le \overline{P_{v,t}^d}, \underline{S_{v,t}} \le S_{v,t} \le \overline{S_{v,t}} \\ S_{v,t} = S_{v,t-1} + \Delta S_{v,t} + \eta^c P_{v,t}^c \Delta t - \frac{\eta^{\mathrm{ref}} P_{v,t}^d \Delta t}{\eta^d} \end{array} \right\} \tag{12}$$

4. Models and algorithms for joint bidding

4.1. Interaction model of DSO and CSOs

In this section, the LDD [37] is used to decompose the global optimal dispatch problem of DSO into the form of an iterative solution between the DSO problem and multiple CSO problems. The global optimal dispatch model of DSO for solving DLMP is established, which has been widely used [20]. In order to guide CSOs to use electricity orderly, the DSO should forecast the market clearing price $\lambda_{t,w}^{\mathrm{DA}}$ and formulate DLMP with the goal of minimizing CSOs operating cost. Eq. (13) is the objective function of DSO w. The first and second items are the purchase cost and the sale profit of CSOs, respectively.

$$\min_{P_{v,t,w}^c, P_{v,t,w}^d} f_w^{DSO} = \sum_{t\in \mathbf{T}} \sum_{v\in \mathbf{V}^w} \left(\lambda_{t,w}^{\mathrm{DA}} P_{v,t,w}^c - \lambda_{t,w}^{\mathrm{DA}} P_{v,t,w}^d\right) \tag{13}$$

$$S_{v,t,w} = S_{v,t-1,w} + \Delta S_{v,t,w} + \eta^c P_{v,t,w}^c - \frac{\eta^{ref} P_{v,t,w}^d}{\eta^d} \tag{14}$$

$$0 \le P_{v,t,w}^c \le \overline{P_{v,t,w}^c}, v \in \mathbf{V}^w \tag{15}$$

$$0 \le P_{v,t,w}^d \le \overline{P_{v,t,w}^d}, v \in \mathbf{V}^w \tag{16}$$

$$\underline{S_{v,t,w}} \le S_{v,t,w} \le \overline{S_{v,t,w}}, v \in \mathbf{V}^w \tag{17}$$

$$P_{v,t,w}^c P_{v,t,w}^d = 0, v \in \mathbf{V}^w \tag{18}$$

$$P_{i,t,w} = \left(P_{i,t,w}^c + P_{i,t,w}^d\right) + P_{i,t,w}^D, \forall i \in \Omega^w \tag{19}$$

$$-\overline{F_{l,w}} \le -\sum_{i\in \Omega^w} D_{l,i} P_{i,t,w} \le \overline{F_{l,w}} : \mu_{l,t}^+, \mu_{l,t}^-, \forall l \in \mathbf{L}^w \tag{20}$$

Notably, different from (3), since the penalty term will be introduced into the objective function later, (18) cannot be ignored. The bilinear constraints are introduced in (18), which makes the problem difficult to solve. Therefore, the big-M method is used to rewrite it in the form of (21). Since DC optimal power flow can provide sufficient accuracy and good convergence when calculating the optimal dispatch problem based on distribution locational price [38], the branch power flow constraint (20) is based on DC power flow.

$$\left\{ \begin{array}{l} 0 \le P_{v,t,w}^c \le \left(1 - \sigma_{v,t,w}\right) M \\ 0 \le P_{v,t,w}^d \le \sigma_{v,t,w} M \end{array} \right. , \sigma_{v,t,w} \in \{0,1\} \tag{21}$$

In the above global optimization model, the DSO has unlimited dispatching rights. Obviously, the CSOs are unwilling to accept this. CSOs want to have the right to make their own energy schedules. Therefore, LDD can be used to decompose the above model so that distributed optimal dispatching can be realized through an iterative solution. However, in the global optimization model, (20) couples the CSOs, which prevents the decomposition of the problem. To solve this problem, the Lagrange auxiliary function is constructed as follows:

$$\begin{aligned} L = &\sum_{t\in \mathbf{T}} \sum_{v\in \mathbf{V}^w} \left(\lambda_{t,w}^{DA} P_{v,t,w}^c - \lambda_{t,w}^{DA} P_{v,t,w}^d\right) \\ &+ \sum_{t\in \mathbf{T}} \sum_{l\in \mathbf{L}^w} \left[\begin{array}{l} \mu_{l,t}^+ \left(-\overline{F_{l,w}} - \sum_{i\in \Omega^w} D_{l,i} P_{i,t,w}\right) \\ +\mu_{l,t}^- \left(-\overline{F_{l,w}} + \sum_{i\in \Omega^w} D_{l,i} P_{i,t,w}\right) \end{array} \right] \end{aligned} \tag{22}$$

It can be seen that (22) is decoupled. Then, its dual function will be decoupled. The dual problem of (13)–(20) is as follows:

$$\begin{aligned} &g\left(\mu_{l,t}^+, \mu_{l,t}^-\right) = \inf_{P_{v,t,w}^c, P_{v,t,w}^d} L\left(P_{v,t,w}^c, P_{v,t,w}^d, \mu_{l,t}^+, \mu_{l,t}^-\right) \\ &s.t.\ \mu_{l,t}^+, \mu_{l,t}^- \ge 0 \end{aligned} \tag{23}$$

After decomposition, the CSO problem is obtained in (24).

$$\begin{aligned} &\min_{P_{v,t,w}^c, P_{v,t,w}^d} \sum_{t\in \mathbf{T}} \sum_{v\in \mathbf{V}^w} \left(\lambda_{t,w}^{DA} + \lambda_{v,t,w}^{DLMP}\right)\left(P_{v,t,w}^c - P_{v,t,w}^d\right) \\ &s.t.\ \lambda_{v,t,w}^{DLMP} = -\mathbf{D}_i^{\mathrm{T}} \boldsymbol{\mu}_t^+ + \mathbf{D}_i^{\mathrm{T}} \boldsymbol{\mu}_t^-, i = \omega(v) \end{aligned} \tag{24}$$

where, $\omega(v)$ is the bus where the CSO v is located.

The dual problem (23) is a nested optimization problem. The outer layer finds the maximum value with respect to the variables $\mu_{l,t}^+$ and $\mu_{l,b}^-$ and the inner layer finds the minimum value with respect to the variables $P_{v,t,w}^c$ and $P_{v,t,w}^d$ for each CSO. The subgradient method [39] can be used to solve the outer optimization problem. Since the dual function $g(\cdot)$ in (23) is a concave function, the subgradient method is used to solve the convex function $-g(\cdot)$. The subgradients S_t of $-g(\cdot)$ are:

$$\left\{ \begin{array}{l} S_{l,t}^{\mu^+} = -\frac{\partial g}{\partial \mu_{l,t}^+} = \overline{F_{l,w}} + \sum_{i\in \Omega^w} D_{l,i} P_{i,t,w} \\ S_{l,t}^{\mu^-} = -\frac{\partial g}{\partial \mu_{l,t}^-} = \overline{F_{l,w}} - \sum_{i\in \Omega^w} D_{l,i} P_{i,t,w} \end{array} \right. \tag{25}$$

Then, multipliers $\mu_{l,t}^+$ and $\mu_{l,t}^-$ are updated iteratively as

$$\mu_{l,t}^{(k+1)} = \max\left\{0, \mu_{l,t}^{(k)} - \alpha S_{l,t}^{\mu,(k)}\right\}, \mu \in \left\{\mu^+, \mu^-\right\} \tag{26}$$

Since the objective function of (23) is differentiable, the convergence of the subgradient method can be guaranteed by choosing an appropriate α for iteration. In (26), $\mu_{l,t}^+$ and $\mu_{l,t}^-$ are the marginal price of network cost caused by congestion when the power flow of branch l exceeds its limit. When the energy schedules reported by the CSOs cannot meet (20), the return values of $\mu_{l,t}^+$ and $\mu_{l,t}^-$ are positive numbers. Otherwise, the return values are zero. The convergence criterion is shown in (27). When the iteration increment is zero, (20) is satisfied.

$$\Delta\mu_{l,t} = \left|\mu_{l,t}^{(k+1)} - \mu_{l,t}^{(k)}\right| \le \varepsilon, \mu \in \left\{\mu^+, \mu^-\right\} \tag{27}$$

4.2. Interaction model between CSOs and TPO

In the independent bidding mode, the clearing price $\lambda_{t,w}^{DA}$ in (24) is forecasted by the CSOs themselves. However, each CSO has a different mastery of market information. It is conceivable that their forecasting of the market clearing price must be biased. Furthermore, the bidding strategies formulated by the fragmented CSOs will cause unnecessary market loss, which leads to inefficient market operation. In this regard, the solution of this paper is as follows: CSOs are affected by the wholesale market and DSOs when they formulate bidding strategies.

$$\begin{aligned}\mathbf{SP1}:\ &\min_{P_{v,t,w}^{CSc},P_{v,t,w}^{CSd}} f_{v,w}^{CSO}=\sum_{t\in\mathbf{T}}\boldsymbol{\Phi}\\ &\boldsymbol{\Phi}=\lambda_{v,t,w}^{DLMP}\left(P_{v,t,w}^{CSc}-P_{v,t,w}^{CSd}\right)\\ &+\pi_{v,t,w}^{c,(k)}\left(P_{v,t,w}^{TPOc,(k)}-P_{v,t,w}^{CSc}\right)+\frac{\rho}{2}\left\|P_{v,t,w}^{TPOc,(k)}-P_{v,t,w}^{CSc}\right\|_2^2\\ &+\pi_{v,t,w}^{d,(k)}\left(P_{v,t,w}^{TPOd,(k)}-P_{v,t,w}^{CSd}\right)+\frac{\rho}{2}\left\|P_{v,t,w}^{TPOd,(k)}-P_{v,t,w}^{CSd}\right\|_2^2 \qquad (28a)\\ s.t.\ &\begin{cases}\lambda_{v,t,w}^{DLMP}=-\mathbf{D}_i^{\mathrm{T}}\boldsymbol{\mu}_t^{+}+\mathbf{D}_i^{\mathrm{T}}\boldsymbol{\mu}_t^{-},i=\omega(v)\\ (14)\text{ - }(17),\ (21)\end{cases} \qquad (28b)\end{aligned}$$

$$\begin{aligned}\mathbf{SP2}:\ &\min_{\kappa_{v,t,w}^{DA}} f^{TPO}=\sum_{t\in T}\sum_{w\in W}\sum_{v\in V^w}\Gamma\\ &\Gamma=\lambda_{t,w}^{DA}\left(P_{v,t,w}^{TPOc}-P_{v,t,w}^{TPOd}\right)\\ &+\pi_{v,t,w}^{c,(k)}\left(P_{v,t,w}^{TPOc}-P_{v,t,w}^{CSc,(k+1)}\right)+\frac{\rho}{2}\left\|P_{v,t,w}^{TPOc}-P_{v,t,w}^{CSc,(k+1)}\right\|_2^2\\ &+\pi_{v,t,w}^{d,(k)}\left(P_{v,t,w}^{TPOd}-P_{v,t,w}^{CSd,(k+1)}\right)+\frac{\rho}{2}\left\|P_{v,t,w}^{TPOd}-P_{v,t,w}^{CSd,(k+1)}\right\|_2^2 \qquad (29a)\\ &s.t.\ S_{v,t,w}=S_{v,t-1,w}+\Delta S_{v,t,w}+\eta^c P_{v,t,w}^{TPOc}\Delta t-\frac{\eta^{ref}P_{v,t,w}^{TPOd}\Delta t}{\eta^d} \qquad (29b)\\ &\underline{S_{v,t,w}}\le S_{v,t,w}\le\overline{S_{v,t,w}},\forall t\in\mathbf{T},\forall v\in\mathbf{V}^w,\forall w\in\mathbf{W} \qquad (29c)\\ &\underline{\kappa_{v,t,w}}\le\kappa_{v,t,w}^{DA}\le\overline{\kappa_{v,t,w}},\forall t\in\mathbf{T},\forall v\in\mathbf{V}^w,\forall w\in\mathbf{W} \qquad (29d)\\ &\text{where}\left\{P_{v,t,w}^{TPOc},P_{v,t,w}^{TPOd}\right\}=\\ &\quad\arg\min_{P_{v,t,w}^{TPOc},P_{v,t,w}^{TPOd},P_{b,t,g}^{G},P_{mn,t}}\left(\begin{array}{l}\sum_{t\in\mathbf{T}}\sum_{g\in\mathbf{TG}}\sum_{b\in\mathbf{N}_{step}}\pi_{b,g}^{G}P_{b,t,g}^{G}\\ -\sum_{t\in\mathbf{T}}\sum_{w\in\mathbf{W}}\sum_{v\in\mathbf{V}^w}\kappa_{v,t,w}^{DA}\left(P_{v,t,w}^{TPOc}-P_{v,t,w}^{TPOd}\right)\end{array}\right) \qquad (29e)\\ &s.t.\ \sum_{g:(g,j)\in\mathbf{TG}}\sum_{b\in\mathbf{N}_{step}}P_{b,t,g}^{G}-\sum_{d:(d,j)\in\mathbf{T}D}P_{t,d}^{D}-\sum_{w\in\mathbf{W}j}\sum_{v\in\mathbf{V}^w}P_{v,t,w}^{TPOc}\\ &\quad+\sum_{w\in\mathbf{W}^j}\sum_{v\in\mathbf{V}^w}P_{v,t,w}^{TPOd}+\sum_{n:(m,n)\in\mathbf{T}L}B_{mn}\left(\theta_{t,m}-\theta_{t,n}\right)=0:\lambda_{t,j}^{DA} \qquad (29f)\\ &0\le P_{v,t,w}^{TPOc}\le\overline{P_{v,t,w}^{TPOc}}:\mu_{v,t,w}^{c-},\mu_{v,t,w}^{c+} \qquad (29g)\\ &0\le P_{v,t,w}^{TPOd}\le\overline{P_{v,t,w}^{TPOd}}:\mu_{v,t,w}^{d-},\mu_{v,t,w}^{d+} \qquad (29h)\\ &-\overline{F_{mn}}\le B_{mn}\left(\theta_{t,m}-\theta_{t,n}\right)\le\overline{F_{mn}}:\mu_{t,mn}^{F-},\mu_{t,mn}^{F+} \qquad (29i)\\ &0\le P_{b,t,g}^{G}\le G_{b,g}:\mu_{b,t,g}^{G-},\mu_{b,t,g}^{G+} \qquad (29j)\\ &-\pi\le\theta_{t,j},\theta_{t,j}\le\pi:\mu_{t,j}^{\theta-},\mu_{t,j}^{\theta+} \qquad (29k)\\ &\theta_{t,j}=0,j=ref:\lambda_t^{ref} \qquad (29l)\end{aligned}$$

where, $\theta_{t,ref}$ is the phase angle of the slack bus in period t.

Based on the decomposition concept of ADMM [40], the bidding problem of CSOs can be divided into two subproblems, i.e., distribution system subproblem SP1 and wholesale market subproblem SP2. SP1 and SP2 are coupled by the CSOs' bidding strategies. The part in (24) related to the bidding cost/benefit of the wholesale market is stripped and then in charge of an independent TPO that can grasp the market information. In the process of interaction, the TPO provides the CSOs with reference schedules on bidding strategy formulation, and the CSOs give feedback after formulating new bidding strategies until both parties reach an agreement. Based on the decomposition mechanism, (24) is divided into SP1 and SP2 as follows. $P_{v,t,w}^{CSc}/P_{v,t,w}^{CSd}$ in SP1 and $P_{v,t,w}^{TPOc}/P_{v,t,w}^{TPOd}$ in SP2 refer to the energy schedule $P_{v,t,w}^{c}/P_{v,t,w}^{d}$.

The update rules and convergence criteria are:

$$\begin{cases}\pi_{v,t,w}^{c,(k+1)}=\pi_{v,t,w}^{c,(k)}+\rho\left(P_{v,t,w}^{TPOc,(k+1)}-P_{v,t,w}^{CSc,(k+1)}\right)\\ \pi_{v,t,w}^{d,(k+1)}=\pi_{v,t,w}^{d,(k)}+\rho\left(P_{v,t,w}^{TPOd,(k+1)}-P_{v,t,w}^{CSd,(k+1)}\right)\end{cases} \qquad (30)$$

$$\begin{cases}\left\|P_{v,t,w}^{TPOc,(k+1)}-P_{v,t,w}^{CSc,(k+1)}\right\|_2^2\le\varepsilon_{pri}\\ \left\|P_{v,t,w}^{CSc,(k+1)}-P_{v,t,w}^{CSc,(k)}\right\|_2^2\le\varepsilon_{dual}\\ \left\|P_{v,t,w}^{TPOd,(k+1)}-P_{v,t,w}^{CSd,(k+1)}\right\|_2^2\le\varepsilon_{pri}\\ \left\|P_{v,t,w}^{CSd,(k+1)}-P_{v,t,w}^{CSd,(k)}\right\|_2^2\le\varepsilon_{dual}\end{cases} \qquad (31)$$

The bilevel model (29) is rewritten through the KKT condition and duality theory [41] in the following form that can be solved directly. Only equality constraints are written here. The remaining inequality constraints are given in Appendix C.

$$\min_{\lambda_{t,w}^{DA}}\left(\begin{array}{l}\sum_{t\in\mathbf{T}}\sum_{g\in\mathbf{TG}}\sum_{b\in\mathbf{N}_{step}}\pi_{b,g}^{G}P_{b,t,g}^{G}-\sum_{t\in\mathbf{T}}\sum_{w\in\mathbf{W}}\lambda_{t,w}^{DA}\sum_{d:(d,j)\in\mathbf{T}D}P_{t,d}^{D}\\ +\sum_{t\in\mathbf{T}}\sum_{g\in\mathbf{TG}}\sum_{b\in\mathbf{N}_{step}}\mu_{b,t,g}^{G+}G_{b,g}+\sum_{t\in\mathbf{T}}\sum_{w:(w,j)\in\mathbf{W}}\left(\mu_{t,w}^{\theta-}+\mu_{t,w}^{\theta+}\right)\pi\\ +\sum_{t\in\mathbf{T}}\sum_{(m,n)\in\mathbf{TL}}\left(\mu_{t,mn}^{F-}+\mu_{t,mn}^{F+}\right)\overline{F_{mn}}\end{array}\right) \qquad (32a)$$

$$s.t.\ \frac{\partial L}{\partial P_{b,t,g}^{G}}=\pi_{b,g}^{G}-\mu_{b,t,g}^{G-}+\mu_{b,t,g}^{G+}-\lambda_{t,g}^{DA}=0 \qquad (32b)$$

$$\frac{\partial L}{\partial P_{v,t,w}^{TPOc}}=-\kappa_{v,t,w}^{DA}+\lambda_{v,t,w}^{DA}-\mu_{v,t,w}^{c-}+\mu_{v,t,w}^{c+}=0 \qquad (32c)$$

$$\frac{\partial L}{\partial P_{v,t,w}^{TPOd}}=\kappa_{v,t,w}^{DA}-\lambda_{v,t,w}^{DA}-\mu_{v,t,w}^{d-}+\mu_{v,t,w}^{d+}=0 \qquad (32d)$$

$$\begin{aligned}&\frac{\partial L}{\partial\theta_{t,m}}=\lambda_{t,m}^{DA}\sum_{n\in\boldsymbol{\omega}_m}B_{mn}+\sum_{n\in\boldsymbol{\omega}_m}B_{mn}\lambda_{t,n}^{DA}-\sum_{n\in\boldsymbol{\omega}_m}B_{mn}\mu_{t,mn}^{F-}\\ &+\sum_{n\in\boldsymbol{\omega}_m}B_{mn}\mu_{t,mn}^{F+}-\mu_{t,m}^{\theta-}+\mu_{t,m}^{\theta+}-\lambda_{t,\mathrm{ref}}=0\end{aligned} \qquad (32e)$$

4.3. Subgradient and ADMM based distributed algorithm

The detailed algorithm is shown in Algorithm 1, with its flowchart shown in Fig. 2. When (27) and (31) are satisfied, the CSOs, TPO and DSO agree on the amount of electricity purchased/sold for each period in the CSOs' bidding strategies. After the day-ahead market opens, the CSOs will participate in the market bidding according to the bid/offer price $\kappa_{v,t,w}^{DA,(K)}$ and the amount of electricity purchased/sold $P_{v,t,w}^{CSc,(K)}$, $P_{v,t,w}^{CSd,(K)}$ agreed upon by the three parties. Then, execute only one round of bid/offer.

4.4. Proof of approximation to social welfare maximization

The social welfare maximization model, i.e., the centralized dispatching model, is shown in (33). The objective is to minimize the total cost of generators. The power system control center has unlimited dispatching power of generators and CSOs. Model (33) is an ideal model, which is difficult to implement in actual scenarios because of the lack of privacy protection, limited computing power and difficult data acquisition.

$$\begin{aligned}&\min f_s=\sum_{t\in\mathbf{T}}\sum_{g\in\mathbf{TG}}\sum_{b\in\mathbf{N}_{step}}\pi_{b,g}^{G}P_{b,t,g}^{G}\\ &s.t.\ (19),(20),(29b),(29c),(29f)\text{ - }(29l)\end{aligned} \qquad (33)$$

Obviously, the constraints in (33) appear in the distribution system subproblem and the wholesale market sub-problem. Moreover, (19) and (20) are satisfied when convergence is reached by multiple iterations between the CSOs and the DSOs, that is, when $\Delta\mu_{l,t}^{+}$ and $\Delta\mu_{l,t}^{-}$ tend to be zero. Assume that the optimal solutions of the centralized dispatching model and the joint bidding model are $\Lambda_{\max}^{*}$ and Λ^{*}, respectively. Then, Λ^{*} satisfies all the constraints of (33), and there exists

$$f_s\left(\Lambda_{\max}^{*}\right)\le f_s\left(\Lambda^{*}\right),\left\{\Lambda_{\max}^{*},\Lambda^{*}\right\}\subseteq\boldsymbol{\Lambda}^{*} \qquad (34)$$

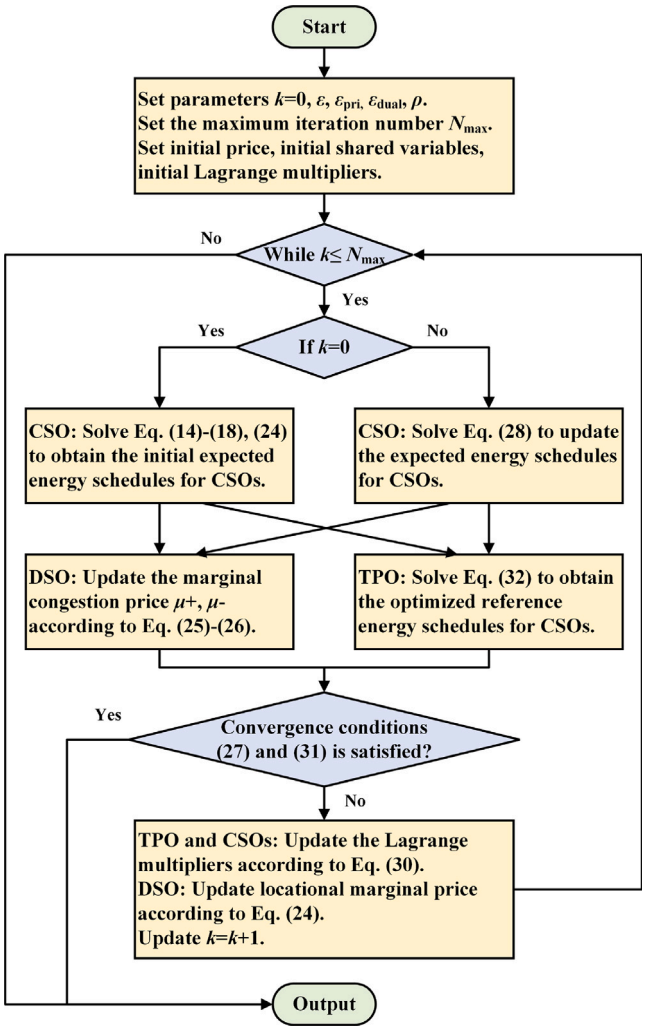

Fig. 2. Flowchart of the Subgradient and ADMM based distributed algorithm.

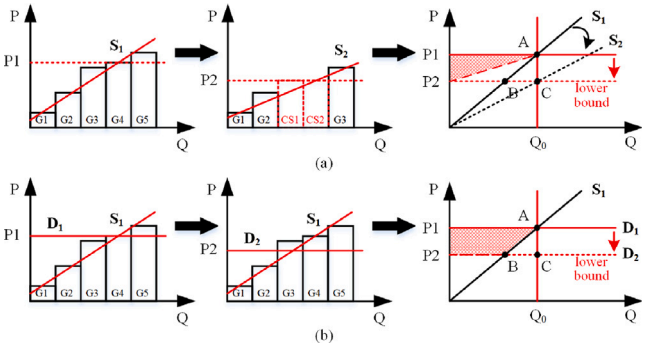

Fig. 3. Social welfare loss schematic.

where $\boldsymbol{\Lambda}^*$ is the set of feasible solutions for (33). The optimal solution Λ^* is the feasible solution of (33), but it is not necessarily the optimal solution. This means that the bidding strategy (including the bid/offer price and the allocation of electricity purchased/sold in each period) of the CSOs obtained from the joint bidding model will inevitably result in market deadweight loss, i.e., social welfare loss. This loss is the result of optimized allocation by the TPO with the objective of minimizing the CSO cluster operating cost. For the convenience of later analysis, the calculation formula of social welfare ψ is given in (35). In the

Algorithm 1 Subgradient and ADMM based distributed algorithm

Initialization:
Set parameters $k = 0$, ε, ε_{pri}, ε_{dual}, ρ.
Set the maximum iteration number N_{max}.
Set price of initial values $\lambda_{v,t,w}^{DLMP,(0)}$ and $\lambda_{t,w}^{DA,(0)}$.
Set shared variables of initial values $P_{v,t,w}^{TPOc,(0)}$ and $P_{v,t,w}^{TPOd,(0)}$.
Set Lagrange multiplier initial values $\pi_{v,t,w}^{c,(0)}$ and $\pi_{v,t,w}^{d,(0)}$.
while $k \le N_{max}$ **do**
  for CSO v, $v \in \mathbf{V}^w, w \in \mathbf{W}$ **do**
    Get $\lambda_{v,t,w}^{DLMP,(k)}$, $\lambda_{t,w}^{DA,(k)}$, $P_{v,t,w}^{TPOc,(k)}$, $P_{v,t,w}^{TPOd,(k)}$, $t \in \mathbf{T}$.
    if $k = 0$ **then**
      Solve (14)-(18) and (24).
    else
      Solve (28).
    end if
    Obtain expected energy schedules $P_{v,t,w}^{CSc,(k+1)}$, $P_{v,t,w}^{CSd,(k+1)}$.
  end for
  for DSO w, $w \in \mathbf{W}$ **do**
    Get $P_{v,t,w}^{CSc,(k+1)}$, $P_{v,t,w}^{CSd,(k+1)}$, $v \in \mathbf{V}^w, w \in \mathbf{W}$.
    Update $\mu_{l,t}^{+,(k+1)}$, $\mu_{l,t}^{-,(k+1)}$ according to (25)-(26).
  end for
  TPO:
  Get $P_{v,t,w}^{CSc,(k+1)}$, $P_{v,t,w}^{CSd,(k+1)}$, $v \in \mathbf{V}^w, w \in \mathbf{W}$.
  Solve (32) to obtain optimized reference energy schedules $P_{v,t,w}^{TPOc,(k+1)}$, $P_{v,t,w}^{TPOd,(k+1)}$, $v \in \mathbf{V}^w, w \in \mathbf{W}, t \in \mathbf{T}$.
  if (27) && (31) **then**
    $k = K$, break.
  else
    for TPO, CSO v, $v \in \mathbf{V}^w, w \in \mathbf{W}$ **do**
      Update $\pi_{v,t,w}^{c,(k+1)}$, $\pi_{v,t,w}^{d,(k+1)}$, $t \in \mathbf{T}$ according to (30).
    end for
    for DSO w, $w \in \mathbf{W}$ **do**
      Calculate locational congestion price $\lambda_{v,t,w}^{DLMP,(k+1)}$, $t \in \mathbf{T}$ according to (24).
    end for
  end if
end while
Output: Final energy schedules $P_{v,t,w}^{CSc,(K)}$, $P_{v,t,w}^{CSd,(K)}$, and bid price $\kappa_{v,t,w}^{DA,(K)}$, $v \in \mathbf{V}^w, w \in \mathbf{W}, t \in \mathbf{T}$.

centralized dispatching mode, the willingness to pay and the actual payment of CSOs are the locational marginal prices. In the joint bidding mode, CSOs will bid as close as possible to the actual clearing price. The consumer surpluses in the two modes can be considered to be zero. Social welfare is equivalent to generator surplus. Therefore, (35) is reasonable.

$$\psi = \sum_{t\in\mathbf{T}}\sum_{w\in\mathbf{W}}\sum_{v\in\mathbf{V}^w}\lambda_{t,w}^{DA}P_{v,t,w}^{TPOd} + \sum_{t\in\mathbf{T}}\left(\sum_{g:(g,j)\in\mathbf{TG}}\lambda_{t,g}^{DA}\sum_{b\in\mathbf{N}_{step}}P_{b,t,g}^{G} - \sum_{g\in\mathbf{TG}}\sum_{b\in\mathbf{N}_{step}}\pi_{b,g}^{G}P_{b,t,g}^{G}\right) \tag{35}$$

During the peak load period, CSOs with discharge capacity hope to sell as much electricity as possible. In this period, the TPO will inevitably guide the CSOs to offer a price less than or equal to the clearing price of the social welfare maximization model. As shown in Fig. 3(a), this result will change the original ranking of the generators, which will reduce the slope of the supply curve. When the demand of the same load is satisfied, the market clearing price will decrease. Although the total generator cost is reduced, the generator surplus is reduced. Then, the shadow area $S_{\Delta AP1P2}$ is the loss of social welfare. However, the TPO can set the necessary lower bound $\underline{\kappa}_{v,t,w}$ to limit $S_{\Delta AP1P2}$ within the predictable and acceptable range to avoid overdepressing the market

clearing price. As the number of generators in the market increases, the decrease in the change in the supply curve slope can also reduce $S_{\Delta \mathrm{AP1}P2}$. Notably, the CSOs will sell more electricity during peak load periods in joint bidding mode. Then, to meet the charging demand of EVs, more electricity needs to be purchased in other periods. This situation leads to an increase in the total generator cost in the nonpeak load period, and the increase is greater than the decrease in the peak load period. This is one of the reasons for (34).

As the number of generators in the electricity market grows, their closely spaced offer prices flatten the supply curve. This weakens the ability of CSOs to profit from strategic discharging in peak load periods. Low discharge bids have less impact on the market clearing price, reducing the associated social welfare loss. In response, CSOs shift to non-peak periods, leveraging market power by submitting lower charging bid prices. These lower bids, as shown in Fig. 3(b), shift the demand curve downward from D_1 to D_2, lowering the market clearing price and allowing CSOs to benefit from reduced electricity purchase costs. However, the lower price and reduced generation output significantly cut generator revenues. The resulting social welfare loss, represented by the parallelogram area S_{ABP1P2}, reflects this decline in generator surplus. To limit this welfare loss and prevent excessive price suppression, the TPO can adjust the minimum bid price $\underline{\kappa}_{v,t,w}$ for CSOs. This ensures the market clearing price supports market stability.

To mathematically derive the market power of CSOs, specifically how their bids influence the clearing price and social welfare, the joint bidding model and the centralized dispatching model are respectively approximated in the following simplified forms. Consider a single bus and a single time period.

$$
\begin{aligned}
&\min_{\kappa_v} \sum_{v\in\mathbf{V}} \lambda\left(p_v-d_v\right)\\
&s.t.\begin{cases}
\underline{\kappa}\le\kappa_v\le\overline{\kappa}\\
\underline{q_v}\le p_v-d_v\le\overline{q_v}\\
\left\{\lambda,p_v,d_v\right\}\in\arg\left\{\min_{G_g,p_v,d_v}\sum_{g\in\mathbf{G}}\pi_g G_g-\kappa_v\left(p_v-d_v\right)\right.\\
\quad s.t.\begin{cases}
\sum_{g\in\mathbf{G}}G_g-\sum_{v\in\mathbf{V}}\left(p_v-d_v\right)=D:\lambda\\
\underline{G_g}\le G_g\le\overline{G_g}\\
\underline{p_v}\le p_v\le\overline{p_v},\underline{d_v}\le d_v\le\overline{d_v}
\end{cases}
\end{cases}
\end{aligned}
\tag{36}
$$

$$
\begin{aligned}
&\min_{G_g,p_v,d_v}\sum_{g\in\mathbf{G}}\pi_g G_g\\
&s.t.\begin{cases}
\sum_{g\in\mathbf{G}}G_g-\sum_{v\in\mathbf{V}}\left(p_v-d_v\right)=D:\lambda\\
\underline{G_g}\le G_g\le\overline{G_g}\\
\underline{p_v}\le p_v\le\overline{p_v},\underline{d_v}\le d_v\le\overline{d_v}\\
\underline{q_v}\le p_v-d_v\le\overline{q_v}
\end{cases}
\end{aligned}
\tag{37}
$$

where π_g and G_g are the offer prices and outputs of generator g, $\forall g\in\mathbf{G}$, and κ_v, p_v, d_v are the bid prices, charging powers, and discharging powers of CSO v, $\forall v\in\mathbf{V}$. Net demand is defined as $q_v:=p_v-d_v$. Physical constraints yield feasible net-demand intervals $q_v\in[\underline{q}_v^{\mathrm{feas}},\overline{q}_v^{\mathrm{feas}}]$, with $\underline{q}_v^{\mathrm{feas}}:=\max\{\underline{q}_v,\underline{p}_v-\overline{d}_v\}$ and $\overline{q}_v^{\mathrm{feas}}:=\min\{\overline{q}_v,\overline{p}_v-\underline{d}_v\}$. The social welfare, as defined in (35), is expressed as:

$$
\psi=\sum_{g\in\mathbf{G}}(\lambda-\pi_g)G_g+\sum_{v\in\mathbf{V}}\lambda d_v. \tag{38}
$$

In the joint bidding model (36), the lower-level problem depends on $\{p_v-d_v\}$ solely through q_v. By eliminating (p_v,d_v), the lower-level problem reduces to a parametric linear program in (G,q):

$$
\begin{aligned}
&\min_{G,q} C(Q)-\sum_{v\in\mathbf{V}}\kappa_v q_v\\
&s.t.\begin{cases}
Q:=\sum_{g\in\mathbf{G}}G_g=D+\sum_{v\in\mathbf{V}}q_i\\
\underline{G_g}\le G_g\le\overline{G_g},\underline{q}_v^{\mathrm{feas}}\le q_v\le\overline{q}_v^{\mathrm{feas}}
\end{cases}
\end{aligned}
\tag{39}
$$

where, $C(Q):=\min\left\{\sum_{g\in\mathbf{G}}\pi_g G_g\mid\sum_{g\in\mathbf{G}}G_g=Q,\ \underline{G_g}\le G_g\le\overline{G_g}\right\}$ is the piecewise-linear convex generation cost function. The KKT conditions, with the power-balance multiplier λ, yield the one-price law:

$$
\lambda\in\partial C(Q),\ q_v=\begin{cases}
\underline{q}_v^{\mathrm{feas}} & \text{if } \lambda>\kappa_v,\\
\in[\underline{q}_v^{\mathrm{feas}},\overline{q}_v^{\mathrm{feas}}] & \text{if } \lambda=\kappa_v,\\
\overline{q}_v^{\mathrm{feas}} & \text{if } \lambda<\kappa_v.
\end{cases}
\tag{40}
$$

Building on the one-price law derived from the lower-level KKT system, the mapping from coordinated bids to the clearing price and to welfare is stated in a stepwise framework. Generators are aggregated into price steps $\{\pi_{(g)}\}_{g=1}^{M}$ with step capacities $C_{(g)}:=\overline{G}_{(g)}-\underline{G}_{(g)}$. Define cumulative capacities $S_k:=\sum_{g=1}^{k}C_{(g)}$ and the base output $G_{\min}:=\sum_g\underline{G_g}$. The supply ladder is the right-continuous nondecreasing function $Q(\lambda)=G_{\min}+S_k$ for $\lambda\in[\pi_{(k)},\pi_{(k+1)})$. Let the current clearing point satisfy $Q=D+\sum_v q_v$ and define $L:=Q-G_{\min}\in(S_{m-1},S_m]$, which fixes the current step index $m:=\min\{k:\ S_k\ge L\}$ and the current locational marginal price $\lambda=\pi_{(m)}$. The downward distance to the lower step is $\delta_m:=L-S_{m-1}\in(0,C_{(m)}]$, which is the net-load reduction required for feasibility at the $(m-1)$-th step under a fixed supply ladder.

Consider any subset $S\subseteq\mathbf{V}$ that rebids from κ_v to κ_v', all other bids unchanged. A reduction of the target price from $\pi_{(m)}$ to $\pi_{(m-1)}$ induces a passive increase of net demand among non-S operators whose bids lie in the interval $(\pi_{(m-1)},\pi_{(m)})$. Define $\Delta F_{-S}:=\sum_{u\notin S}\left(q_u(\pi_{(m-1)})-q_u(\pi_{(m)})\right)\ge 0$. At the target price $\pi_{(m-1)}$, the realizable net-load reduction that subset S can mobilize is $\Delta F_S^{\mathrm{targ}}:=\sum_{v\in S}\left(q_v(\pi_{(m-1)})-\underline{q}_v^{\mathrm{feas}}\right)_+$, subject to $\kappa_v'\le\pi_{(m-1)}$ so that the members of S remain on the low-net-demand side imposed by the one-price law.

Proposition 1. *Let $\lambda=\pi_{(m)}$. There exist bids $\{\kappa_v'\}_{v\in S}$ with $\kappa_v'\le\pi_{(m-1)}$ such that the post-rebid clearing price satisfies $\lambda'\le\pi_{(m-1)}$ if and only if $\Delta F_S^{\mathrm{targ}}\ge\delta_m+\Delta F_{-S}$.*

Proof. By the infimum characterization of the price, define $\Lambda[F]:=\inf\{\lambda:\ Q(\lambda)\ge F(\lambda)\}$, thus $\lambda'=\Lambda[F^{\mathrm{new}}]\le\pi_{(m-1)}$ is equivalent to $F^{\mathrm{new}}(\pi_{(m-1)})\le Q(\pi_{(m-1)})=G_{\min}+S_{m-1}$. At $\pi_{(m-1)}$, all $v\in S$ with $\kappa_v'\le\pi_{(m-1)}$ are dispatched at $q_v=\underline{q}_v^{\mathrm{feas}}$, hence $F^{\mathrm{new}}(\pi_{(m-1)})=F^0(\pi_{(m-1)})-\Delta F_S^{\mathrm{targ}}$. Decompose the baseline gap: $F^0(\pi_{(m-1)})-Q(\pi_{(m-1)})=\left(F^0(\pi_{(m)})-Q(\pi_{(m-1)})\right)+\left(F^0(\pi_{(m-1)})-F^0(\pi_{(m)})\right)$, where the first term equals δ_m and the second equals $\Delta F_{-S}+\Delta F_S^0$ with $\Delta F_S^0:=\sum_{v\in S}\left(q_v(\pi_{(m-1)})-q_v(\pi_{(m)})\right)\ge 0$. Since $\Delta F_S^{\mathrm{targ}}\ge\Delta F_S^0$, the inequality $F^{\mathrm{new}}(\pi_{(m-1)})\le Q(\pi_{(m-1)})$ is equivalent to $\Delta F_S^{\mathrm{targ}}\ge\delta_m+\Delta F_{-S}$. Necessity and sufficiency follow. □

A bid-adjusted one-step leverage index consistent with the threshold is

$$
\mathcal{L}_S^{(1)}=\mathbf{1}_{\{\kappa_v'\le\pi_{(m-1)}\ \forall v\in S\}}\cdot\min\left\{1,\ \frac{\Delta F_S^{\mathrm{targ}}}{\delta_m+\Delta F_{-S}}\right\}. \tag{41}
$$

where, The index $\mathcal{L}_S^{(1)}\in[0,1]$ quantifies the ratio between the subset's realizable adjustable net-load and the net-load threshold required to move the price down by one step. It equals one precisely when the subset can reduce the price to at most $\pi_{(m-1)}$. Multi-step reductions to $\pi_{(m-K)}$ are obtained by summing per-step requirements. The condition is $\kappa_v'\le\pi_{(m-K)}$ for all $v\in S$ and $\Delta F_S^{\mathrm{targ}}\ge\sum_{j=1}^{K}(\delta_{m-j+1}+\Delta F_{-S}^{(m-j+1\to m-j)})$, $\Delta F_{-S}^{(m-j+1\to m-j)}:=\sum_{u\notin S}(q_u(\pi_{(m-j)})-q_u(\pi_{(m-j+1)}))$.

Proposition 2. *Let $(Q^{\mathrm{J}},\lambda^{\mathrm{J}},p^{\mathrm{J}},d^{\mathrm{J}},q^{\mathrm{J}})$ and $(Q^{\mathrm{C}},\lambda^{\mathrm{C}},p^{\mathrm{C}},d^{\mathrm{C}},q^{\mathrm{C}})$ be feasible solutions of the joint bidding model and of the centralized dispatching model under identical physical limits. Define $Q_{\max}:=\min\{\sum_g\overline{G}_g,\ D+\sum_v\overline{q}_v^{\mathrm{feas}}\}$. Let $\bar{\lambda}$ denote a known price cap. Then $|\psi^{\mathrm{J}}-\psi^{\mathrm{C}}|\le Q_{\max}|\lambda^{\mathrm{J}}-\lambda^{\mathrm{C}}|+\bar{\lambda}\sum_v((\overline{p}_v-\underline{p}_v)+(\overline{q}_v^{\mathrm{feas}}-\underline{q}_v^{\mathrm{feas}}))$, and, in the special case where $\sum_v d_v^{\mathrm{J}}=\sum_v d_v^{\mathrm{C}}$, $|\psi^{\mathrm{J}}-\psi^{\mathrm{C}}|\le Q_{\max}|\lambda^{\mathrm{J}}-\lambda^{\mathrm{C}}|$.*

Proof. Social welfare satisfies $\psi=\lambda Q-C(Q)+\lambda\sum_v d_v=C^*(\lambda)+\lambda\sum_v d_v$, where C^* is the Fenchel conjugate of C and $\lambda\in\partial C(Q)$ implies

$C^*(\lambda) = \lambda Q - C(Q)$. For any two feasible solutions, $|\psi^J - \psi^C| \le |C^*(\lambda^J) - C^*(\lambda^C)| + |\lambda^J \sum_v d_v^J - \lambda^C \sum_v d_v^C|$. Since $\partial C^*(\lambda) \subset [0, Q_{\max}]$, the function C^* is $Q_{\max}$-Lipschitz, hence $|C^*(\lambda^J) - C^*(\lambda^C)| \le Q_{\max}|\lambda^J - \lambda^C|$.

Write $d_v = p_v - q_v$. Then $|\lambda^J \sum_v d_v^J - \lambda^C \sum_v d_v^C| \le \bar{\lambda} \sum_v |p_v^J - p_v^C| + \bar{\lambda} \sum_v |q_v^J - q_v^C|$. Each absolute difference is bounded by the corresponding feasible interval, that is $|p_v^J - p_v^C| \le \overline{p}_v - \underline{p}_v$ and $|q_v^J - q_v^C| \le \overline{q}_v^{\text{feas}} - \underline{q}_v^{\text{feas}}$. Summation over v gives the residual term and yields the general bound. If $\sum_v d_v^J = \sum_v d_v^C$, the second term is zero and the price-gap specialization follows. □

The term $|\lambda^J - \lambda^C|$ can be controlled by the bid vector κ^J as follows. Let $\mathcal{A}^C := \{v : q_v^C \in (\underline{q}_v^{\text{feas}}, \overline{q}_v^{\text{feas}})\}$ be the set of CSOs that are interior in the centralized solution. Assume the active-set pattern remains stable when comparing to the joint-bidding outcome, so that every $v \in \mathcal{A}^C$ is also interior in the joint-bidding solution. By the one-price condition, for any $v \in \mathcal{A}^C$, $\lambda^J = \kappa_v^J$. Hence, $|\lambda^J - \lambda^C| \le \max_{v \in \mathcal{A}^C} |\kappa_v^J - \lambda^C|$. Substitution into the above bound yields $|\psi^J - \psi^C| \le Q_{\max} \max_{v \in \mathcal{A}^C} |\kappa_v^J - \lambda^C| + \bar{\lambda} \sum_v ((\overline{p}_v - \underline{p}_v) + (\overline{q}_v^{\text{feas}} - \underline{q}_v^{\text{feas}}))$.

Remark: Propositions 1 and 2 provide the mathematical description of Fig. 3. Proposition 1 demonstrates that, when CSOs possess sufficient regulation capacity, they can influence the market clearing price by adjusting their bid/offer prices. This highlights the market power of CSOs as price-makers, allowing them to strategically shift the equilibrium price through coordinated bidding under the TPO's guidance. In essence, if the aggregate adjustable net demand from a subset of CSOs meets or exceeds the required threshold for price reduction (considering passive adjustments from other operators), the clearing price can be lowered by one or more steps, as quantified by the leverage index $\mathcal{L}_S^{(1)}$. This intuitive insight underscores how CSOs with large flexible capacities, such as those aggregated from EVs, can act as pivotal players in imperfect markets, potentially mitigating disordered competition. Proposition 2 establishes that the upper bound on social welfare loss is directly tied to the CSOs' bid/offer prices. Specifically, the loss is minimized and potentially approaches zero when all CSOs' bids align with the clearing price from the centralized dispatching model, which represents the theoretical social optimum. This bound is derived from the Lipschitz continuity of the generation cost function and the feasible intervals of charging/discharging powers, providing a practical metric for evaluating bidding deviations. Intuitively, any mismatch between joint bidding outcomes and centralized solutions leads to inefficiencies, such as suboptimal resource allocation or unnecessary congestion costs. By coordinating CSOs' bid/offer prices, such as adjusting their price boundaries, the proposed mode effectively controls this loss within a small range. Proposition 1 empowers CSOs with strategic leverage, while Proposition 2 bounds the downside risks, ensuring the joint bidding mode is both feasible and welfare-enhancing in real-world applications.

5. Case study

This paper initially conducts simulations in the IEEE-9 bus transmission system and the IEEE-33 bus distribution system, which represent a small-scale transmission and distribution system, with data and network topology detailed in Appendix B. Four CSOs, exhibiting varied energy usage behaviors, are located at buses 12, 19, 23, and 29 within the distribution system, while ten identical distribution systems are connected at buses 5, 7, and 9 in the transmission system. Thereafter, to evaluate the effectiveness and scalability of the proposed algorithm in large-scale transmission and distribution systems, simulations are performed in the IEEE-118 bus transmission system and the IEEE-33 bus distribution system, as illustrated in Fig. 12. By modifying the basic load data of the transmission system, the proportion of charging capacity to the total electricity load during the peak charging period is more than 20%, which reflects the large scale and market share of the CSOs. The whole cycle consists of 96 time periods, starting at 8 a.m. and ending at 8 a.m. the next day. The bid/offer price range is [10,130] $/MW. The models are coded in MATLAB environment with YALMIP interface and solved by GUROBI 12.0 toolbox in Windows 10 operating system under the hardware environment that Intel(R) Core(TM) i7-4710HQ CPU@2.50 GHz, 8 GB RAM.

5.1. Comparison with independent bidding mode

In this section, the competitive independent bidding mode where each CSO goes on its own is compared. The competitive bidding bilevel optimization model under the unified clearing price mode in Appendix C is used to analyze the independent bidding strategies of CSOs and their impact on the market clearing price. Because of the many CSOs participating in wholesale market bidding, CSOs forecast the bid/offer price and energy schedule of each CSO with difficulty when formulating bidding strategies. Therefore, in the simulation, CSOs only forecast the data of competitors in the local distribution system, and other CSOs are considered in the basic load. The local verification function of DSOs remains, and the wholesale market clearing model is shown in Appendix C. Taking CSO3 in any distribution system as an example, the results of the independent bidding mode and joint bidding mode are shown in Figs. 4(a)–4(b) and Figs. 4(c)–4(d), respectively. DAc/DAd/Rc/Rd represent the amount of electricity purchased/sold in the day-ahead bidding strategies and actual clearing results. DAP/CP represents the bid/offer price of the CSO and actual clearing price.

Comparing the results of the two modes shows that the CSOs cannot forecast the market clearing price accurately under the independent bidding mode, which leads to the bid/offer price being higher or lower than the market clearing price in some periods. According to (32c) and (32d), when the bid/offer price is higher/lower than the market clearing price, the MO will clear according to the maximum amount of electricity purchased/sold reported by a CSO. Only when a CSO forecasts the market clearing price accurately can the deviation between the actual clearing results and the day-ahead bidding strategies be small. However, the degree of deviation will still be affected by the bid/offer prices from other CSOs. After the intervention of the TPO, which can more accurately grasp the market information, the CSOs can optimize their bidding strategies according to the reference energy schedules from the TPO and reach a consensus on the bid/offer price, as shown in Fig. 5. In period [1,20], since CSO1 and CSO4 do not purchase or sell electricity and the maximum amount of electricity purchased/sold reported by them in this period is zero, they only bid/offer at the lowest price. CSO2 and CSO3 need to purchase electricity, so they reach a consensus on the bid price and report it at the price given by the TPO. It can be seen that the guiding role of the TPO has realized price consensus among local CSOs. Furthermore, the accurate estimation of the market clearing price makes the actual clearing results basically consistent with the expectation of CSOs, which avoids the social welfare loss caused by disorderly competition.

5.2. Comparison with centralized dispatching mode

In this section, (33) is used to calculate the electricity purchased/sold amount of CSOs and clearing price under centralized dispatching mode. The results are compared with those of the joint bidding mode. Take four CSOs in any distribution system as an example, as shown in Figs. 6 and 7. TPOc/TPOd and SMc/SMd represent the amount of electricity purchased/sold under the joint bidding mode and centralized dispatching mode, respectively. TPO-CP/SM-CP represents the market clearing price under the joint bidding mode and centralized scheduling mode. In Fig. 6, the results of the two modes are consistent in most periods. However, since the centralized dispatching model only considers the optimal total amount of electricity purchased/sold in each period, there are multiple solutions to the electricity purchase/sale allocation of CSOs. Therefore, the results of the same CSO deviate during a few periods under the two modes in Fig. 6, but the total amount of electricity purchased/sold in each period is basically the same under

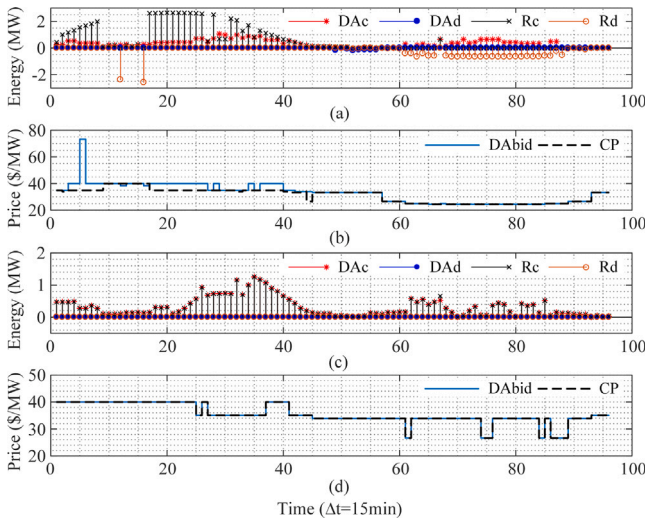

Fig. 4. Results of CSO3 in independent bidding mode and joint bidding mode.

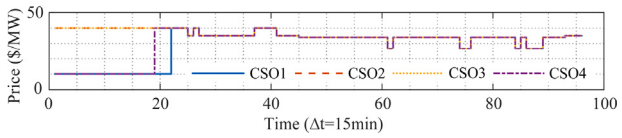

Fig. 5. Bid/offer prices of CSOs in the same distribution system under joint bidding mode.

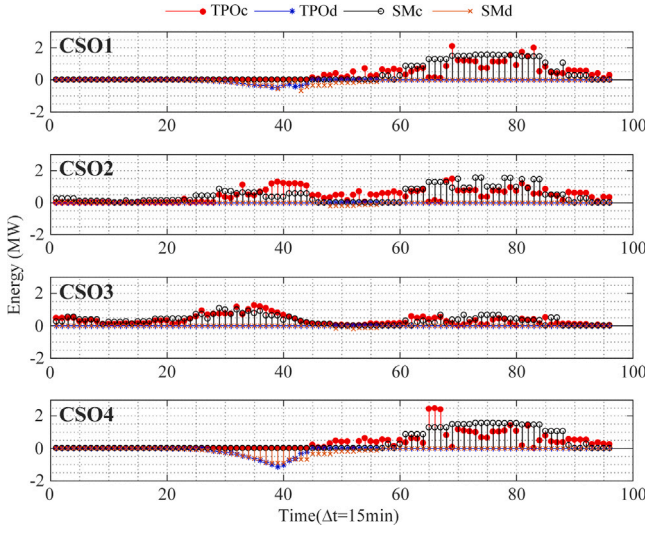

Fig. 6. Comparison of the electricity purchased/sold amount.

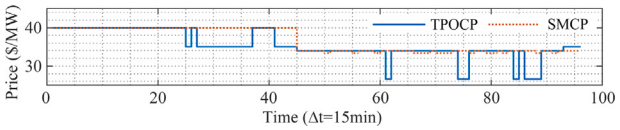

Fig. 7. Comparison of market clearing prices.

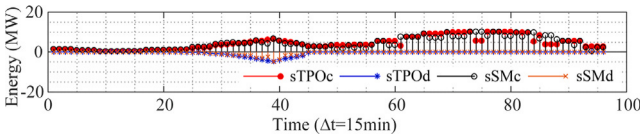

Fig. 8. Total amount of electricity purchased/sold under the two modes.

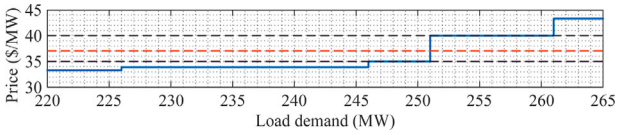

Fig. 9. Supply curve in wholesale market.

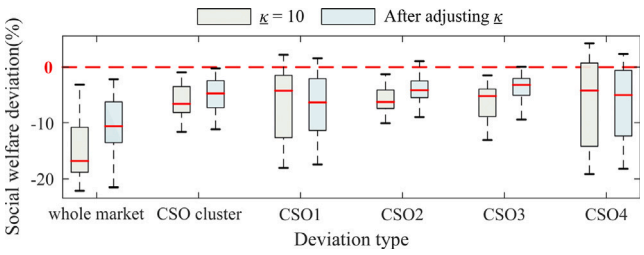

Fig. 10. Distribution of social welfare deviation between joint bidding mode and centralized dispatching mode (The calculation methods of deviation is $\frac{(A-B)\times 100\%}{B}$, where A, B are the results of joint bidding mode and centralized dispatching mode, respectively).

Table 1
Social welfare and bidding cost comparison of two modes.

Bidding mode	Centralized dispatching	Joint bidding	Difference
Social welfare ($)	89006.8	80471.1	859.6
Total generator cost ($)	130832.0	130931.3	−99.3
Bidding cost of CSOs($)			
CSO1	952.8	962.5	−9.7
CSO2	1561.2	1477.5	83.7
CSO3	1218.4	1111.7	106.7
CSO4	731.6	770.0	−38.4

Table 2
Social welfare loss under different lower bounds during period [30, 40].

Lower bound ($/MW)	$\underline{\kappa} = 10$	$\underline{\kappa} = 37$	$\underline{\kappa} = 40$
Social welfare ($)	8047.2	8285.2	8288.8
Social welfare loss ($)	859.6	621.6	618.0

Table 3
Consuming time of each iteration.

Iteration number	1	2	3	4	5	6	7
Consuming time (s)	509	531	569	579	449	427	348

the two modes in Fig. 8. The difference in clearing price between the two modes in Fig. 7 is mainly reflected in the period when CSOs sell electricity centrally. The clearing price is affected by the bid/offer price of CSOs during period [30,40] and the allocation of electricity purchased during period [60,90].

Table 1 shows that the joint bidding mode has caused social welfare loss. Fig. 9 shows that when the load during period [30, 40] is greater than 251 MW, the CSOs can seize part of the electricity sale directly from the generator whose offer price is $40/MW as long as they report an offer price of any value between [35, 40)$/MW. If the sum of the electricity sold by the CSOs and the generators that have obtained the sale right can meet the load demand during this period, the market clearing price will be reduced from $40/MW to the offer price reported by the CSOs. Social welfare losses result from this. However, Table 2

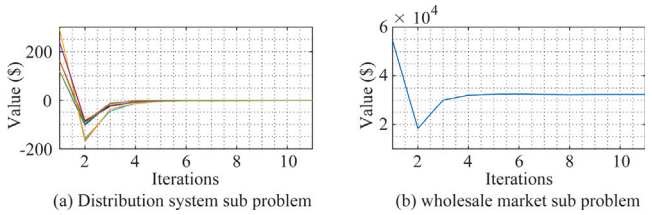

Fig. 11. Convergence curve of algorithm iteration process.

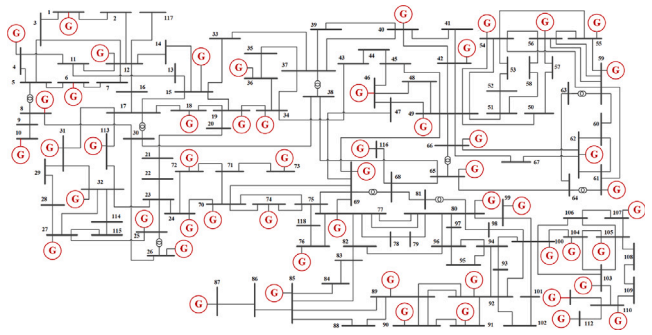

Fig. 12. IEEE 118-bus system.

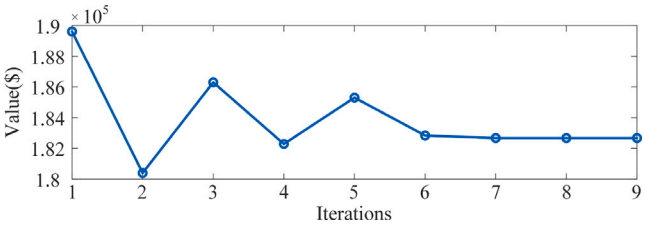

Fig. 13. Convergence curve of IEEE 118-bus system simulation.

shows that when the TPO increases the lower bound of the bid/offer price, the social welfare loss decreases as the lower bound increases from \$10/MW to \$40/MW (equal to the clearing price of the centralized dispatching mode). The minimum value of \$618.0 is reached when the lower bound is \$40/MW. Therefore, the amount of social welfare loss can be controlled by changing the lower bound of the bid/offer price. When the lower bound of the bid/offer price is set according to the clearing price curve of the centralized dispatching mode, the social welfare loss is the smallest. In addition, in Fig. 9, when the number of generators and their generation blocks increases, the number of blocks in the load interval [245, 251] MW increases, which can reduce the impact of CSOs on social welfare loss after they obtain the electricity sale right.

Further, the load data of the UK power grid [42] from January 1, 2019 to March 31, 2019 are selected to be converted into standard unitary values for calculation. As shown in Fig. 10, when the lower bounds $\underline{\kappa}$ = \$10/MW, the minimum and maximum social welfare deviations of the whole market between the two modes are −3.0% and −22.1%, respectively. The deviation values are concentrated in the interval [−10.8%, −18.7%]. After the lower bounds $\underline{\kappa}$ during period [30, 40] are adjusted upward, the minimum and maximum deviations are reduced to −2.1% and −21.5%, respectively. The deviation values are concentrated in the interval [−6.2%, −13.5%]. This shows that the joint bidding mode can approach the maximum social welfare, and the deviation can be further reduced by adjusting the lower bound of the bid/offer price with reference to the clearing price of the centralized scheduling model. More importantly, for the CSO cluster, it can be seen that the deviation of the cluster total benefit between the two modes is concentrated in the interval [−2.4%, −7.2%], and the minimum deviation is only −0.2%. In some days, the benefits of CSO1, 2 and 4 under the joint bidding mode are better than that under the centralized dispatching mode.

5.3. Convergence and advantages of the algorithm

The iteration step $\alpha = 1 \times 10^{-4}$ and penalty coefficient $\rho = 1$ are set in the simulation. The time complexity of the ADMM algorithm is $O(n^2)$, which depends on the number n of CSOs participating in the joint bidding [40]. For the subgradient method, the algorithm will converge as long as an appropriate step size α is chosen. Since the convergence process is not monotonic, the time complexity can be approximately considered as $O(\varepsilon)$, which depends on the convergence accuracy ε [39]. Then, the time complexity of the proposed algorithm depends on the one with higher time complexity. Fig. 11 shows that the objective functions of the wholesale market subproblem and distribution system subproblem stabilize after four iterations and converge after six iterations. The consuming time of the first seven iterations is shown in Table 3. Although a large number of binary variables in the decision-making model of the TSO greatly increases the consuming time, the consuming time of single iteration decreases as the value of the objective function tends to converge. In terms of iteration number and time, it can be considered that the proposed algorithm can be used in day-ahead bidding and has good convergence. In addition, the algorithm can obtain the global optimal solution through a small amount of information communication and multiple iterations among CSOs, DSOs and the TPO.

In Tables 1 and 2, there is a difference between social welfare under the optimal solution of the joint bidding mode and the centralized dispatching mode. However, the difference is small and controllable. Moreover, because of the distributed characteristics of the joint bidding mode, CSOs can complete the interaction in the actual market as long as they have information receiving and transmitting devices. The distributed algorithm can give the CSO initiative and avoid many problems, such as user information leakage and high computing pressure in the centralized dispatching mode.

5.4. Simulation analysis in large-scale power systems

To assess the effectiveness of the proposed algorithm in large-scale power systems, this section replaces the previously used IEEE 9-bus system with the IEEE 118-bus system, as illustrated in Fig. 12. The IEEE 118-bus system consists of 54 generators, with each load bus connected to 10 distribution systems. Each distribution system includes four distinct types of megawatt-scale CSs, as shown in Fig. B1, resulting in a total of 396 CSs. The base load data of the IEEE 118-bus system is modified to achieve an EV penetration of approximately 20%.

Fig. 13 presents the convergence curve of the wholesale market subproblem. The algorithm converges by the seventh iteration, demonstrating that it maintains a fast convergence rate even as the system scale increases. In Fig. 14, simulations are conducted using historical load data from the UK power grid, as described in Section 5.2. The simulation results indicate that, while the maximum social welfare deviation in the wholesale market reaches 30.43%, it is primarily concentrated within the range [0.00%, 19.43%]. Through TPO, the joint bidding mode achieves social welfare equivalent to the centralized dispatching mode on certain days. The social welfare deviation of the CSO cluster reaches a maximum of 13.61%, with most values distributed in the range [0.00%, 5.49%]. Notably, the social welfare deviation of the four types of CSOs is positive on some days, indicating that the joint bidding mode allows CSOs to gain profits through market power while closely approximating optimal social welfare. To minimize social welfare losses, these profits are kept within a small range.

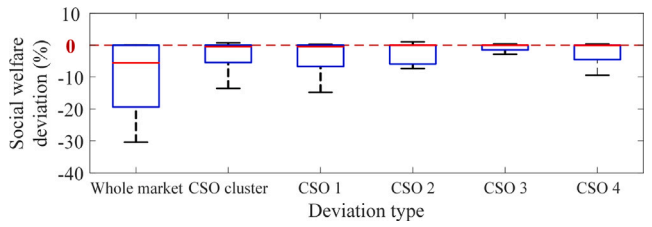

Fig. 14. Distribution of social welfare deviation under joint bidding mode.

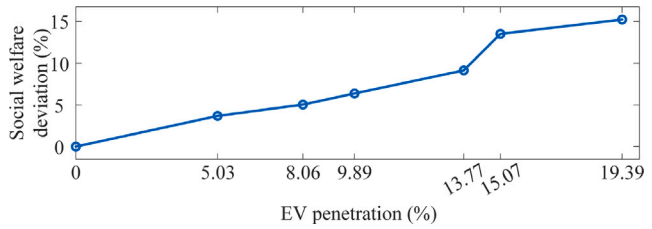

Fig. 15. Relationship between social welfare deviations and EV penetration.

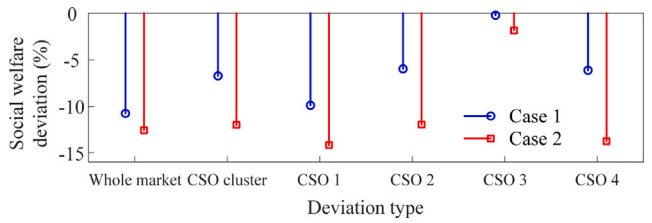

Fig. 16. Impact of CSOs' individual profit motives on social welfare.

Furthermore, Fig. 15 illustrates the relationship between social welfare deviation and EV penetration. As the EV penetration increases, the social welfare deviation gradually rises. At an EV penetration of 19.39%, the social welfare deviation reaches 15.24%. This is attributed to the increased market power of the CSO cluster as EV penetration grows. With stronger market power, it becomes challenging for the TPO to significantly reduce social welfare losses by adjusting the bid price boundaries of CSOs, although the losses remain within an acceptable range.

5.5. Impact of CSOs' individual profit motives on social welfare

In the proposed joint bidding model, it is assumed that all CSOs formulate their energy schedules based on a standardized optimization objective. However, some CSOs may include additional terms related to charging/discharging profits or costs in their optimization objectives to maximize profits, resulting in the submission of non-truthful expected energy schedules to the TPO. To analyze the impact of this behavior on social welfare losses, in this section, 25% of CSOs are selected, and quadratic terms for charging utility and discharging cost are added to their optimization objectives [43], as described below:

$$\Phi' = \left(\alpha_{v,w} P_{v,t,w}^{CSd} + \beta_{v,w}\left(P_{v,t,w}^{CSd}\right)^2\right) - \left(a_{v,w} P_{v,t,w}^{CSc} - b_{v,w}\left(P_{v,t,w}^{CSc}\right)^2\right)$$

where, Φ' represents the additional term incorporated into the optimization objective of CSO v (28a), with the first term corresponding to the discharging cost and the second term to the charging utility, as detailed in [43]. The coefficients $\alpha_{v,w}$ and $\beta_{v,w}$ denote the discharging cost coefficients, while $a_{v,w}$ and $b_{v,w}$ represent the charging utility coefficients.

Fig. 16 compares the social welfare losses before and after the inclusion of additional terms in the optimization objectives of selected CSOs. In Case 1, all CSOs adhere to the standardized objective function, serving as the baseline scenario. In Case 2, 25% of CSOs incorporate the modified objective Φ', simulating non-truthful bidding behavior. The results show that when these CSOs privately modify their optimization objectives and misreport their true energy schedules, the whole market's social welfare loss increases from 10.75% to 12.60%, the CSO cluster's social welfare loss rises from 6.73% to 12.03%, and the social welfare loss for individual CSOs also increases. This occurs because the altered optimization objectives cause the energy schedules submitted to the TPO to deviate from actual demand, shifting the optimal solution of the joint bidding model and consequently impacting market clearing outcomes and social welfare maximization. However, the incremental increase in social welfare loss remains relatively limited, demonstrating the robustness of the proposed joint bidding model. The TPO, through coordinated bidding strategies for multi-region charging stations, effectively controls social welfare losses within a small range, ensuring market efficiency and stability.

6. Discussion

Through multi-region coordination by the TPO for CSOs with local coordination by DSOs, the proposed joint bidding mode presents a promising strategy for enhancing social welfare in electricity markets characterized by imperfect competition and asymmetric information. This section provides an in-depth exploration of three critical aspects: the legal and operational authority of the TPO, the advantages for adopting the distributed algorithm, and the framework's adaptability to diverse market designs and regulatory environments.

6.1. Legal and operational authority of the TPO

The TPO's legal authority can be anchored in existing regulatory frameworks that support aggregation and coordination in electricity markets. In the United States, FERC Order No. 2222 [8], issued in September 2020, permits distributed energy resources, including CSOs, to participate in electricity markets through aggregation. This order implicitly supports entities like the TPO by encouraging non-discriminatory access and coordination, potentially classifying it as a regulated aggregator under MO oversight. In China, provincial regulations (e.g., Hunan's non-profit dispatching organization [24]) allow for centralized disclosure of market data to mitigate disorderly bidding. The TPO could operate under similar mandates. The TPO is designed as a nonprofit entity, distinct from profit-driven CSOs, and operates under the supervision of the MO. The MO, which aligns with Independent System Operators (ISOs) such as PJM or CAISO in deregulated markets, oversees the process. The TPO plays a central role in the joint bidding framework, acting as a coordinator for CSOs under the supervision of the MO to facilitate coordinated bidding while minimizing the social welfare losses caused by information asymmetry, as outlined in Section 2. Its operational framework involves iterative sharing of optimized reference schedules $P_{v,t,w}^{TPOc}$, $P_{v,t,w}^{TPOd}$ with CSOs, derived from the wholesale market subproblem SP2 (29), which incorporates generator offers $\pi_{b,g}^{G}$ and network constraints (29i)–(29l). To enable effective coordination, the MO discloses aggregated but sensitive market data, such as generator offers $\pi_{b,g}^{G}$ and complete network parameters B_{mn}, $\overline{F_{mn}}$, to the TPO under strict confidentiality, ensuring this information is not shared with CSOs to safeguard individual privacy of generators and maintain market fairness.

A robust governance structure is essential to enhance the TPO's realism. A multi-stakeholder governance board, comprising MO representatives, DSOs, CSO associations, regulatory authorities (e.g., FERC or China's National Energy Administration), and independent auditors, is proposed to oversee the TPO's operations. This board would manage decision-making, conduct annual audits, and ensure compliance with antitrust laws (e.g., U.S. Sherman Antitrust Act [44] or China's Anti-Monopoly Law [45]) to prevent market manipulation. Decisions on

coordination strategies could require a two-thirds majority vote, with regulators holding veto power in cases of suspected collusion. For instance, if a CSO consistently fails to reach consensus during the iterative process despite multiple rounds of reference schedule adjustments, the board could investigate potential strategic non-compliance or technical issues. Alternatively, if a CSO agrees to a consensus bid/offer price $\kappa^{DA}_{v,t,w}$ but subsequently submits a significantly different bid in the day-ahead market, the board could review the case to assess whether market rules were violated, though enforcement would rely on market-driven consequences, such as suboptimal clearing prices, financial losses from missed opportunities, or congestion-related penalties, rather than direct penalties.

The TPO's data access is strictly limited to non-confidential, aggregated inputs to ensure fairness. It does not handle sensitive CSO data such as individual EV states $s_{e,t}$, $X_{e,t}$ in (1)–(7) or proprietary forecasting models, complying with privacy regulations like the EU's General Data Protection Regulation (GDPR) [46], California's Consumer Privacy Act [47], and China's Personal Information Protection Law [48]. Data exchange occurs via secure, encrypted protocols, with only energy schedules and dual variables π_c, π_d in (30) shared iteratively, as validated by the distributed algorithm's convergence.

Unlike centralized coordinators, the TPO does not enforce bidding strategies. Its influence stems from iterative consensus-building, where CSOs adjust their expected energy schedules $P^{CSc}_{v,t,w}$, $P^{CSd}_{v,t,w}$ in (28) based on TPO reference schedules $P^{TPOc}_{v,t,w}$, $P^{TPOd}_{v,t,w}$ in (29), achieving a schedule consensus that reduces social welfare deviation to within an acceptable range. If a CSO opts out post-consensus, it faces market-driven outcomes (e.g., suboptimal clearing due to congestion), not TPO penalties. This voluntary approach aligns with FERC's emphasis on market-driven participation.

6.2. Advantages for adopting the distributed algorithm

The distributed algorithm decomposes the global optimization into subproblems, SP1 for distribution-level coordination (28) and SP2 for wholesale-level optimization (29), exchanging only anonymized energy schedules and dual variables. This contrasts with centralized models, which require aggregating all CSO data, including charging/discharging power boundaries $P^{c}_{v,t}$, $P^{d}_{v,t}$ and capacity-related parameters $\underline{S_{v,t}}$, $\overline{S_{v,t}}$, $\Delta S_{v,t}$ from (12), into a single optimization managed by the MO. While the MO typically safeguards this data, the centralized approach increases the risk of privacy breaches due to the concentration of sensitive information, particularly if third-party coordinators or inadequate security measures are involved. For example, in a network with a large number of CSOs across multiple regions, a data breach or lack of anonymization could expose regional load patterns, potentially violating GDPR Article 25 on data minimization. The distributed method mitigates this by using penalty terms and Lagrange multipliers to enforce consensus without revealing underlying data, ensuring compliance with privacy laws through decentralized processing.

The parallel structure of the algorithm enables efficient scaling to large networks. In the case study, convergence occurs in 7 iterations for the IEEE-118 bus system. Centralized models, however, solve monolithic problems (e.g., (28) for all CSOs), leading to computational intractability with hundreds of CSOs. The ADMM decomposition distributes the workload across CSOs and TPO, as shown in Section 4.2, supporting scalability without exponential growth. Moreover, the algorithm aligns with single-round bidding rules in markets like PJM and CAISO, avoiding the iterative revisions required by game-theoretic models such as GNE [28]–[30]. GNE relies on long-term games with full information sharing (e.g., via KKT conditions or diagonalization), necessitating repeated bid adjustments that disrupt operational timelines. For instance, adding a new CSO could reset the equilibrium, requiring months to stabilize. The ADMM approach, however, achieves consensus pre-market through short iterations, submitting final bids in one round. This reduces collusion risks, as players cannot repeatedly manipulate prices, and complies with FERC Order No. 719 [6], which limits iterative market clearing.

Centralized coordination assumes a single entity optimizes all schedules with the objective of maximizing system-wide welfare, achieving optimal social welfare under ideal conditions. However, it requires CSOs to report extensive private information, and its computational complexity escalates exponentially with the number of participants, rendering it intractable for large-scale systems with numerous CSOs. GNE models target optimal utility through equilibrium but demand unrealistic data sharing [33], with deviations from maximum welfare remaining unanalyzed. In contrast, the distributed algorithm is capable of approaching the optimal social welfare while avoiding issues such as privacy breaches, computational intractability in large networks, and regulatory non-compliance due to excessive information demands.

6.3. Adaptability to diverse market environments

The joint bidding framework is fundamentally designed for a day-ahead (DA) market with locational marginal pricing (LMP), as reflected in the unified clearing model (29e)–(29l), where the TPO coordinates CSOs to submit single-round bids/offer prices $\kappa^{DA}_{v,t,w}$ based on reference schedules $P^{TPOc}_{v,t,w}$, $P^{TPOd}_{v,t,w}$. This LMP structure, embedded in the wholesale market subproblem SP2 (29), calculates LMP $\lambda^{DA}_{t,j}$ for each bus j, incorporating transmission constraints such as branch flows (29f) and capacities (29i). In contrast, PJM's DA market, managed by its ISO, determines LMPs as an outcome of the market clearing process based on aggregated CSO bids/offers, without preemptive schedule guidance. The proposed framework's TPO, by providing reference schedules derived from aggregated market data (e.g., generator offers and transmission parameters), offers a proactive coordination mechanism that could enhance PJM's approach. This could be integrated by expanding the ISO's role to include TPO-like functions, using the distributed algorithm to inform CSO bidding strategies and align with localized grid conditions. The ADMM penalties facilitate convergence on energy schedules between the TPO and CSOs, enforcing consistency in the coordinated schedules, thereby maintaining the distributed algorithm's focus on schedule coordination.

Beyond PJM, the framework's adaptability extends to other DA markets employing LMP and diverse regulatory contexts, leveraging its distributed architecture. In markets like ERCOT [49], which utilize LMP in their DA operations, the TPO can support large-scale coordination by accommodating the region's extensive network and variable renewable generation, leveraging the distributed algorithm's scalability to manage numerous CSOs effectively. For example, ERCOT's DA market could benefit from the TPO's coordination to streamline bidding across its decentralized grid, reducing social welfare deviations. In zonal DA markets, such as those under EU directives [7], the framework can aggregate CSOs by zone, adjusting the wholesale market subproblem SP2 (29) to optimize zonal LMP averages. The TPO would use zone-specific aggregated data to generate reference schedules, with ADMM penalties ensuring convergence across zones. This aligns with EU policies promoting consumer participation, as the minimal data exchange complies with GDPR. For instance, in Germany's DA market, the TPO could coordinate CSOs to balance renewable integration, reducing social welfare deviations similar to the UK results in Section 5.2.

In the U.S., under FERC Order No. 2222, the TPO could operate as a regulated aggregator within the ISO framework, enhancing DA market participation of distributed resources like CSOs. The governance structure would include ISO and regulatory representatives to enforce anti-manipulation rules, ensuring fair coordination and compliance with market standards. In China's emerging DA market, the TPO could be state-affiliated, mirroring Hunan's non-profit dispatching model, providing reference schedules based on aggregated operational data to CSOs while minimizing private data exchange. In Australia's National Electricity Market (NEM) DA market [50], the TPO could collaborate

with the Australian Energy Market Operator (AEMO), integrating renewable uncertainty into generation $P^{G}_{b,t,g}$ via scenario-based forecasts, enhancing welfare under AEMO's rules.

Despite its versatility, the framework faces limitations in DA markets with high variability. The iteration convergence criterion may slow with large CSO cohorts, necessitating optimization of the step size α in (26) or penalty coefficient ρ in (30). Additionally, integrating risk-aware bidding into the wholesale market subproblem SP2 (29) [32], e.g., accounting for random generation from renewables, could enhance DA performance, though it increases computational demands.

7. Conclusions

In this paper, the day-ahead joint bidding model of CSOs under the coordination of the TPO and local DSOs is established based on the LDD method and ADMM decomposition mechanism, and the distributed algorithm based on the subgradient method and ADMM is designed to solve the model. By comparing the simulation results of the independent bidding mode, centralized dispatching mode and joint bidding mode, the following conclusions are obtained:

(1) In the independent bidding mode, since CSOs have difficulty grasping market information and cannot forecast the market clearing price accurately in the short term, they cannot report the bid/offer price as close to the clearing price as possible in the bidding. As a result, the actual clearing result is far from the estimated result. In the joint bidding mode, the TPO analyzes the impact of the joint bidding on the clearing price on the basis of grasping the market information and then coordinates the bidding strategies of CSOs. Through coordination, the CSOs at the same transmission system bus can reach a price consensus on the bid/offer price. This avoids severe deviation of actual clearing results from estimates due to blind bidding;

(2) In the joint bidding mode, the lower offer price of CSOs will reduce the generator surplus, resulting in social welfare loss. However, the loss can be controlled within the acceptable range by adjusting the lower bound of the bid/offer price and introducing more power generators into the market, thus approaching social welfare maximization. The joint bidding mode realizes the Kaldor-Hicks improvement on the CSO cluster benefits, which can attract more CSOs to join;

(3) The distributed algorithm based on the subgradient method and ADMM has good convergence. By separating the constraints of the distribution system and wholesale market clearing from the CSO model, the CSOs can use market power through the TPO while maintaining their initiatives without affecting the obtainment of global optimal solutions. The joint bidding mode based on a distributed algorithm is easy to implement in the actual market. Only one round of bids/offers is needed, which will help to improve market efficiency.

Future research will extend this work in the following directions: (1) investigating the joint bidding problem in dynamic markets with the entry and exit of new participants, such as energy storage and wind power; (2) incorporating uncertainties in the bidding process by extending the model to intra-day and real-time markets to evaluate its performance in multi-timeframe environments, enhancing applicability and robustness against dynamic uncertainties like renewable energy fluctuations through integrating forecast uncertainties into intra-day adjustments and real-time balancing mechanisms; (3) developing a multi-agent game model based on the proposed method to analyze optimal bidding strategies under varying market boundary conditions; (4) examining the impact of communication delays and infrequent information updates on coordination efficiency, incorporating communication network constraints or adaptive update mechanisms; and (5) analyzing the environmental impact of the joint bidding model, such as carbon emission reductions through optimized charging patterns, to enhance its value in sustainable electricity markets.

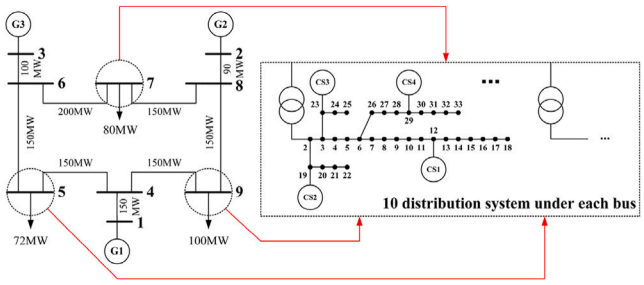

Fig. B.1. Schematic diagram of network topology.

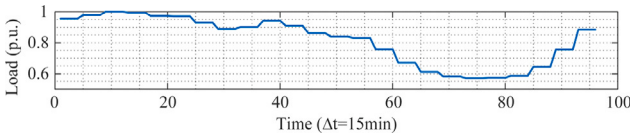

Fig. B.2. Load baseline.

CRediT authorship contribution statement

Gaojunjie Li: Writing – original draft, Methodology. **Huiying Li:** Resources, Data curation. **Fuzhang Wu:** Funding acquisition, Conceptualization. **Xiangpeng Zhan:** Project administration, Investigation. **Xiang Gao:** Visualization, Validation.

Declaration of competing interest

The authors declare that they have no known competing financial interests or personal relationships that could have appeared to influence the work reported in this paper.

Appendix A

Compare two charging modes of EVs.
Mode 1: charging with P^{c}_{1} and discharging with P^{d}_{1} at the same time.
Mode 2: charging with P^{c}_{2} only.
Then, when the scheduling period ends, there is

$$P^{c}_{1}\eta\Delta t - \frac{P^{d}_{1}\Delta t}{\eta} = P^{c}_{2}\eta\Delta t \tag{A.1}$$

In this case, assume the electricity price is c, the Mode 1 cost is $c\left(P^{c}_{1}-P^{d}_{1}\right)\Delta t$, and the Mode 2 cost is $cP^{c}_{2}\Delta t$. Since the charge and discharge efficiency $\eta<1$, there is

$$c\left(P^{c}_{1}-P^{d}_{1}\right)\Delta t = c\left[P^{c}_{2}+P^{d}_{1}\left(\frac{1}{\eta^{2}}-1\right)\right]\Delta t > cP^{c}_{2}\Delta t \tag{A.2}$$

Therefore, Mode 2 is more economical. The EVs choose to charge only rather than charge and discharge at the same time. It can also be proven that EVs choose to discharge only.

Appendix B

See Figs. B.1–B.3 and Table B.1.

Appendix C

Independent bidding mode:

$$\min_{\kappa^{DA}_{t,w}} f^{CSO}_{t,w} = \sum_{t\in\mathbf{T}}\left(\lambda^{DA}_{t,w}+\lambda^{DLMP}_{i,t,w}\right)\left(P^{c}_{t,w}-P^{d}_{t,w}\right) \tag{C.1}$$
$$s.t.\ (29b)\text{ - }(29l)$$

Table B.1
Price offer and capacity of generation unit blocks.

Generators	G1	G2	G3
Block 1	(0,40]/15[a]	(0,40]/15	(0,40]/20
Block 2	(40,60]/24.4	(40,60]/20	(40,60]/26.7
Block 3	(60,80]/33.9	(60,80]/25	(60,80]/33.3
Block 4	(80,85]/43.3	(80,85]/30	(80,85]/40
Block 5	(85,90]/52.8	(85,90]/35	(85,90]/46.7
Block 6	(90,95]/62.2	(90,95]/40	(90,95]/53.3
Block 7	(95,100]/71.7	(95,100]/45	(95,100]/60

[a] $(X,Y]/Z$: $(X,Y]$ is block intervals (MW). Z is the offer price ($/MW).

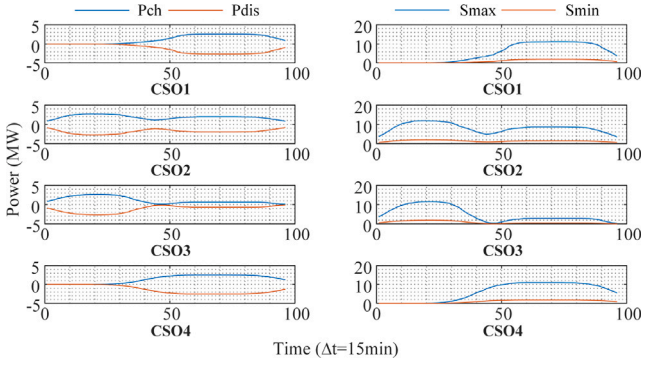

Fig. B.3. Generalized energy storage parameters for four CSOs.

In the existing clearing mechanism of day-ahead wholesale market [13], the market operator clears the day-ahead charge and discharge power according to the bid/offer price of each CSO. On the one hand, only based on the price signal, the energy demands of the CSOs cannot be accurately reflected. Due to the multiplicity of solutions for linear programming (29e)–(29l), there are infinite combinations of final market clearing results. On the other hand, it can be seen from (32c)–(C.2) and (32d)–(C.5) that the bidding strategy of the CSO will be accepted only when its bid/offer price is exactly equal to the locational marginal price. Otherwise, when the reported price is higher/lower than the locational marginal price, it will be cleared according to the maximum charging/discharging power reported by the CSO. This will make the market clearing results greatly deviate from CSO's expectation, which is caused by the limitations of the existing market clearing model.

$$0 \le P^{c}_{v,t,w} \le M\chi^{c-}_{v,t,w}, 0 \le \mu^{c-}_{v,t,w} \le M\left(1-\chi^{c-}_{v,t,w}\right) \tag{C.2}$$

$$0 \le \overline{P^{c}_{v,t,w}} - P^{c}_{v,t,w} \le M\chi^{c+}_{v,t,w}, 0 \le \mu^{c+}_{v,t,w} \le M\left(1-\chi^{c+}_{v,t,w}\right) \tag{C.3}$$

$$0 \le P^{d}_{v,t,w} \le M\chi^{d-}_{v,t,w}, 0 \le \mu^{d-}_{v,t,w} \le M\left(1-\chi^{d-}_{v,t,w}\right) \tag{C.4}$$

$$0 \le \overline{P^{d}_{v,t,w}} - P^{d}_{v,t,w} \le M\chi^{d+}_{v,t,w}, 0 \le \mu^{d+}_{v,t,w} \le M\left(1-\chi^{d+}_{v,t,w}\right) \tag{C.5}$$

$$\begin{aligned} &0 \le B_{mn}\left(\theta_{t,m}-\theta_{t,n}\right)+F^{u}_{mn} \le M\chi^{F-}_{t,mn}, \\ &0 \le \mu^{F-}_{t,mn} \le M\left(1-\chi^{F-}_{t,mn}\right) \end{aligned} \tag{C.6}$$

$$\begin{aligned} &0 \le F^{u}_{mn} - B_{mn}\left(\theta_{t,m}-\theta_{t,n}\right) \le M\chi^{F+}_{t,mn}, \\ &0 \le \mu^{F+}_{t,mn} \le M\left(1-\chi^{F+}_{t,mn}\right) \end{aligned} \tag{C.7}$$

$$0 \le P^{G}_{b,t,g} \le M\chi^{G-}_{b,t,g}, 0 \le \mu^{G-}_{b,t,g} \le M\left(1-\chi^{G-}_{b,t,g}\right) \tag{C.8}$$

$$0 \le G_{b,g} - P^{G}_{b,t,g} \le M\chi^{G+}_{b,t,g}, 0 \le \mu^{G+}_{b,t,g} \le M\left(1-\chi^{G+}_{b,t,g}\right) \tag{C.9}$$

$$0 \le \theta_{t,j} + \pi \le M\chi^{\theta-}_{t,j}, 0 \le \mu^{\theta-}_{t,j} \le M\left(1-\chi^{\theta-}_{t,j}\right) \tag{C.10}$$

$$0 \le \pi - \theta_{t,j} \le M\chi^{\theta+}_{t,j}, 0 \le \mu^{\theta+}_{t,j} \le M\left(1-\chi^{\theta+}_{t,j}\right) \tag{C.11}$$

where M is an arbitrarily large (not infinite) positive number. χ is a binary variable.

Therefore, in this paper, it is assumed that the market operator tracks the expected charge and discharge power reported by the CSO as much as possible while clearing according to the bid/offer price. The method is to minimize the power deviation based on the KKT system (C.12e) of the market clearing problem, that is, on the basis of meeting the market clearing conditions, market operator will ensure that the clearing results are as close to the expected value of each CSO as possible. Furthermore, the clearing model based on stationary point method is established, which is a mixed integer linear programming problem shown in (C.12).

$$\min_{P^{c}_{v,t,w},P^{d}_{v,t,w}} \sum_{t\in\mathbf{T}}\sum_{v\in\mathbf{V}^{w}}\sum_{w\in\mathbf{W}} \left(P^{c}_{v,t,w}-P^{c,\exp}_{v,t,w}\right)^2 + \left(P^{d}_{v,t,w}-P^{d,\exp}_{v,t,w}\right)^2 \tag{C.12a}$$

$$s.t.\ 0 \le P^{c}_{v,t,w} \le \sigma^{c}_{v,t,w}\overline{P^{c}_{v,t,w}}, 0 \le P^{d}_{v,t,w} \le \sigma^{d}_{v,t,w}\overline{P^{d}_{v,t,w}} \tag{C.12b}$$

$$\sigma^{c}_{v,t,w} + \sigma^{d}_{v,t,w} \le 1, \sigma^{c}_{v,t,w}, \sigma^{d}_{v,t,w} \in \{0,1\}, \tag{C.12c}$$

$$\kappa^{DA}_{v,t,w} = \kappa^{DA*}_{v,t,w} \tag{C.12d}$$

$$\mathbb{C}^{KKT} = \{(29f),(29l),(32a)\text{-}(32e),(C.2)\text{-}(C.11)\} \tag{C.12e}$$

where $P^{c,\exp}_{v,t,w}$ and $P^{d,\exp}_{v,t,w}$ are the expected charging and discharging power reported by CSO v in period t, respectively. $\kappa^{DA*}_{v,t,w}$ is the bid/offer price reported by the CSO after coordination.

By substituting the bid/offer price and energy schedules of the CSOs coordinated by the TPO into the above clearing model, the clearing results approaching the maximum social welfare can be obtained.

Data availability

Data will be made available on request.

References

[1] International Energy Agency. Global EV outlook 2024. 2024, [Online] URL https://www.iea.org/reports/global-ev-outlook-2024.
[2] Electrek. Tesla opens new world's largest supercharger station. 2020, [Online] URL https://electrek.co/2020/12/31/.
[3] Parag Y, Sovacool BK. Electricity market design for the prosumer era. Nat Energy 2016;1(4):16032.
[4] Zhao J-W, Zhang H-L, Wang C. Distributed state-of-charge and power balance estimation for aggregated battery energy storage systems with EV aggregators. Energy 2024;305:132193.
[5] Singh A, Sampath LPMI, Nguyen DH, Gooi HB, Nguyen HD. A multi-agent framework for P2P energy trading with EV aggregators supporting V2X services. IEEE Trans Veh Technol 2024;73(12):18548–59.
[6] Federal Energy Regulatory Commission. Order No. 719-B. 2002, [Online] URL https://www.ferc.gov/sites/default/files/2020-06/OrderNo.719-B.pdf.
[7] European Union. Energy efficiency directives. 2012, [Online] URL https://eur-lex.europa.eu/legal-content/EN/TXT/PDF/?uri=CELEX:32012L0027&qid=1608892652796&from=EN.
[8] Federal Energy Regulatory Commission. Order No. 2222. 2020, [Online] URL https://www.ferc.gov/sites/default/files/2020-09/E-1_0.pdf.
[9] Chen Y, Hu S, Xie S, Zheng Y, Hu Q, Yang Q. Optimal dynamic pricing of fast charging stations considering bounded rationality of users and market regulation. IEEE Trans Smart Grid 2024;15(4):3950–65.
[10] Wang M, Li X, Dong C, Mu Y, Jia H, Li F. Day-ahead optimal bidding for a retailer with flexible participation of electric vehicles. IEEE Trans Smart Grid 2023;14(2):1482–94.
[11] Paredes A, Aguado JA, Essayeh C, Xia Y, Savelli I, Morstyn T. Stacking revenues from flexible DERs in multi-scale markets using tri-level optimization. IEEE Trans Power Syst 2024;39(2):3949–61.
[12] Cui Y, Hu Z, Wan Y, Li J, Shao C, Bao Z, Duan X. A distributed week-ahead scheduling method for the charging / discharging of plug-in electric vehicles integrated into the grid. CSEE J Power Energy Syst 2024;1–11.
[13] Ruiz C, Conejo AJ. Pool strategy of a producer with endogenous formation of locational marginal prices. IEEE Trans Power Syst 2009;24(4):1855–66.
[14] Qi L, Wang L, Ding J, Ni W. Pricing design for EV platoon charging network with hybrid traffic flows. IEEE Trans Transp Electrification 2025;11(1):1431–41.
[15] Mirheli A, Hajibabai L. Charging network design and service pricing for electric vehicles with user-equilibrium decisions. IEEE Trans Intell Transp Syst 2023;24(3):2888–902.

[16] Ji H, Zheng Y, Yu H, Zhao J, Song G, Wu J, Li P. Asymmetric bargaining-based SOP planning considering peer-to-peer electricity trading. IEEE Trans Smart Grid 2025;16(2):942–56.
[17] Beykirch M, Bott A, Janke T, Steinke F. The value of probabilistic forecasts for electricity market bidding and scheduling under uncertainty. IEEE Trans Power Syst 2024;39(6):6986–97.
[18] Chen Y, Zheng Y, Hu S, Xie S, Yang Q. Optimal operation of fast charging station aggregator in uncertain electricity markets considering onsite renewable energy and bounded EV user rationality. IEEE Trans Ind Informatics 2024;20(11):13384–95.
[19] Perez-Diaz A, Gerding E, McGroarty F. Coordination and payment mechanisms for electric vehicle aggregators. Appl Energy 2018;212:185–95.
[20] Zhao Z, Liu Y, Guo L, Bai L, Wang Z, Wang C. Distribution locational marginal pricing under uncertainty considering coordination of distribution and wholesale markets. IEEE Trans Smart Grid 2023;14(2):1590–606.
[21] Li G, Yang J, Wu F, Zhu X, Xu J, Sun Y. Electric vehicle aggregation in a PV-battery charging station: A contract-based approach. IEEE Trans Power Syst 2024;39(2):2475–90.
[22] Perez-Diaz A, Gerding EH, McGroarty F. Catching cheats: Detecting strategic manipulation in distributed optimisation of electric vehicle aggregators. J Artificial Intelligence Res 2020;67:437–70.
[23] Perez-Diaz A. Coordination of electric vehicle aggregator participation in the day-ahead market. In: Proceedings of the 17th international conference on autonomous agents and multiAgent systems. 2018, p. 1768–9.
[24] Development and Reform Commission of Hunan Province. Trial scheme of green power transaction of electric vehicles in hunan in 2021. 2021, [Online] URL http://fgw.hunan.gov.cn.
[25] Dehghani M, Ghiasi M, Niknam T, Kavousi-Fard A, Shasadeghi M, Ghadimi N, Taghizadeh-Hesary F. Blockchain-based securing of data exchange in a power transmission system considering congestion management and social welfare. Sustainability 2020;13(1):90.
[26] Tómasson E, Hesamzadeh MR, Wolak FA. Optimal offer-bid strategy of an energy storage portfolio: A linear quasi-relaxation approach. Appl Energy 2020;260:114251.
[27] Li G, Yang J, Wu F, Zhu X, Ke S, Li Y. A market framework for a 100 market. IEEE Trans Sustain Energy 2023;14(3):1569–84.
[28] Xia Y, Xu Q, Ding Y, Shi L, Wu F. Generalized Nash equilibrium analysis for peer-to-peer transactive energy market considering coupling distribution network constraints. IEEE Trans Ind Informatics 2024;20(6):8125–37.
[29] Zhong W, Xie S, Xie K, Yang Q, Xie L. Cooperative P2P energy trading in active distribution networks: An MILP-based Nash bargaining solution. IEEE Trans Smart Grid 2021;12(2):1264–76.
[30] Kim H, Lee J, Bahrami S, Wong VWS. Direct energy trading of microgrids in distribution energy market. IEEE Trans Power Syst 2020;35(1):639–51.
[31] Chen Y, Zhao C, Low SH, Wierman A. An energy sharing mechanism considering network constraints and market power limitation. IEEE Trans Smart Grid 2023;14(2):1027–41.
[32] Xiao D, Peng Z, Lin Z, Zhong X, Wei C, Dong Z, Wu Q. Incorporating financial entities into spot electricity market with renewable energy via holistic risk-aware bilevel optimization. Appl Energy 2025;398:126449.
[33] Jiang K, Liu N, Yan X, Xue Y, Huang J. Modeling strategic behaviors for genco with joint consideration on electricity and carbon markets. IEEE Trans Power Syst 2023;38(5):4724–38.
[34] Wang C, Xu H, Guo C, Zhang X, Qiao Y. Multi-stakeholder behavior analysis of shared energy storage market based on evolutionary game. CSEE J Power Energy Syst 2024;1–12.
[35] Ligao J, Yang J, Li H, Shao L, Xiao Y, Qin S, Zhu X, Wu F. A day-ahead market clearing mechanism for nodal carbon intensity control using the flexibility of charging stations. Int J Electr Power Energy Syst 2023;147:108907.
[36] Li Y, Wu J, Liu B, Ai X, Hu J. Integration of prosumers' flexibilities in distribution network operation. In: 2018 2nd IEEE conference on energy internet and energy system integration. IEEE; 2018, p. 1–6.
[37] Boyd S, Xiao L, Mutapcic A, Mattingley J. Notes on decomposition methods. Notes EE364B, Stanf Univ 2007;635:1–36.
[38] Li F, Bo R. DCOPF-based LMP simulation: Algorithm, comparison with ACOPF, and sensitivity. IEEE Trans Power Syst 2007;22(4):1475–85.
[39] Boyd S, Xiao L, Mutapcic A. Subgradient methods. Lect Notes EE392o, Stanf Univ Autumn Quart 2003;2004(01).
[40] Boyd S, Parikh N, Chu E, Peleato B, Eckstein J, et al. Distributed optimization and statistical learning via the alternating direction method of multipliers. Found Trends® Mach Learn 2011;3(1):1–122.
[41] Ruiz C, Conejo AJ. Pool strategy of a producer with endogenous formation of locational marginal prices. IEEE Trans Power Syst 2009;24(4):1855–66.
[42] ENTSO-E. Power statistics. 2025, [Online] URL https://www.entsoe.eu/data/power-stats/.
[43] Li G, Yang J, Hu Z, Zhu X, Xu J, Sun Y, Zhan X, Wu F. A novel price-driven energy sharing mechanism for charging station operators. Energy Econ 2023;118:106518.
[44] National Archives. Sherman anti-trust act (1890). 1890, [Online] URL https://www.archives.gov/milestone-documents/sherman-anti-trust-act.
[45] National People's Congress of the People's Republic of China. Anti-monopoly law of the People's Republic of China. 2008, [Online] URL https://english.www.gov.cn/services/doingbusiness/202102/24/content_WS6035f1ddc6d0719374af97b6.html.
[46] gdpr-infoeu. General data protection regulation (GDPR). 2018, [Online] URL https://gdpr-info.eu/.
[47] Office of the Attorney General, California. California consumer privacy act (CCPA). 2018, [Online] URL https://oag.ca.gov/privacy/ccpa.
[48] National People's Congress of the People's Republic of China. Personal information protection law of the People's Republic of China. 2021, [Online] URL https://personalinformationprotectionlaw.com/.
[49] Electric Reliability Council of Texas. Electric reliability council of texas. 2025, [Online] URL https://www.ercot.com/.
[50] Australian Energy Market Operator. National electricity market (NEM). 2025, [Online] URL https://www.aemo.com.au/energy-systems/electricity/national-electricity-market-nem.